Mantle dynamics beneath the Pacific Northwest and the generation of voluminous back-arc volcanism

Geochemistry Geophysics Geosystems G3

Published by AGU and the Geochemical Society

Article
Volume 13, Number 1
21 August 2012
Q0AN01, doi:10.1029/2012GC004189
ISSN: 1525-2027

Mantle dynamics beneath the Pacific Northwest and the generation of voluminous back-arc volcanism

Maureen D. Long
Department of Geology and Geophysics, Yale University, PO Box 208109, New Haven, Connecticut 06520, USA (maureen.long@yale.edu)

Christy B. Till
Department of Earth, Atmospheric, and Planetary Sciences, Massachusetts Institute of Technology, Cambridge, Massachusetts 02139, USA

Now at United States Geological Survey, Menlo Park, California 94025, USA

Kelsey A. Druken
Graduate School of Oceanography, University of Rhode Island, Narragansett, Rhode Island 02882, USA

Department of Terrestrial Magnetism, Carnegie Institution of Washington, Washington, D. C. 20015, USA

Richard W. Carlson
Department of Terrestrial Magnetism, Carnegie Institution of Washington, Washington, D. C. 20015, USA

Lara S. Wagner
Department of Geological Sciences, University of North Carolina, Chapel Hill, North Carolina 27599, USA

Matthew J. Fouch and David E. James
Department of Terrestrial Magnetism, Carnegie Institution of Washington, Washington, D. C. 20015, USA

Timothy L. Grove
Department of Earth, Atmospheric, and Planetary Sciences, Massachusetts Institute of Technology, Cambridge, Massachusetts 02139, USA

Nicholas Schmerr
Department of Terrestrial Magnetism, Carnegie Institution of Washington, Washington, D. C. 20015, USA

Planetary Geodynamics Laboratory, NASA Goddard Space Flight Center, Greenbelt, Maryland 20771, USA

Chris Kincaid
Graduate School of Oceanography, University of Rhode Island, Narragansett, Rhode Island 02882, USA

[1] The Pacific Northwest (PNW) has a complex tectonic history and over the past ~17 Ma has played host to several major episodes of intraplate volcanism. These events include the Steens/Columbia River flood basalts (CRB) and the striking spatiotemporal trends of the Yellowstone/Snake River Plain (Y/SRP) and High Lava Plains (HLP) regions. Several different models have been proposed to explain these features, which variously invoke the putative Yellowstone plume, rollback and steepening of the Cascadia slab, extensional processes in the lithosphere, or a combination of these. Here we integrate seismologic, geodynamic, geochemical, and petrologic results from the multidisciplinary HLP project and associated analyses of EarthScope USArray seismic data to propose a conceptual model for post-20 Ma mantle dynamics beneath the PNW and the relationships between mantle flow and surface tectonomagmatic activity. This model invokes rollback subduction as the main driver for mantle flow beneath the PNW beginning at ~20 Ma. A major pulse of upwelling due to slab rollback and upper plate extension and consequent melting produced the Steens/CRB volcanism, and continuing trench migration enabled mantle upwelling and hot, shallow melting beneath the HLP. An additional buoyant mantle upwelling is required to explain the Y/SRP volcanism, but subduction-related processes may well have played a primary role in controlling its timing and location, and this upwelling likely continues today in some form. This conceptual model makes predictions that are broadly consistent with seismic observations, geodynamic modeling experiments, and petrologic and geochemical constraints.

Components: 14,200 words, 9 figures.

Keywords: intraplate volcanism; mantle dynamics; mantle upwelling; slab rollback; subduction.

Index Terms: 8120 Tectonophysics: Dynamics of lithosphere and mantle: general (1213); 8170 Tectonophysics: Subduction zone processes (1031, 3060, 3613, 8413); 8415 Volcanology: Intra-plate processes (1033, 3615).

Received 24 April 2012; **Revised** 12 July 2012; **Accepted** 14 July 2012; **Published** 21 August 2012.

Long, M. D., C. B. Till, K. A. Druken, R. W. Carlson, L. S. Wagner, M. J. Fouch, D. E. James, T. L. Grove, N. Schmerr, and C. Kincaid (2012), Mantle dynamics beneath the Pacific Northwest and the generation of voluminous back-arc volcanism, *Geochem. Geophys. Geosyst.*, *13*, Q0AN01, doi:10.1029/2012GC004189.

Theme: Genesis of continental intraplate magmatism - the example from the Pacific Northwest, USA

1. Introduction

[2] The Pacific Northwest (PNW) region of the United States has experienced a complicated tectonic and volcanic history over the past 50 Ma [e.g., *Christiansen and Lipman*, 1972; *Humphreys and Coblentz*, 2007]. The tectonic setting is dominated by the presence of the subducting Juan de Fuca and Gorda plates to the west; these plates are remnants of the long-lived Farallon plate, which has been subducting beneath North America for the past ~150 Ma [e.g., *Severinghaus and Atwater*, 1990]. The Juan de Fuca plate is subducting beneath North America at a rate of 30 mm/yr to the northeast, and is narrowing along strike as the Mendocino triple junction continues to migrate north. Simultaneously, the trench is rolling back at a rate of ~35 mm/yr in a Pacific hot spot reference frame [*Schellart et al.*, 2008]. At 17 Ma, the character of volcanism in this area changed dramatically (Figure 1), beginning with the massive outpourings of the Steens and Columbia River flood basalts. Subsequent tectonomagmatic activity in the PNW has been dominated by volcanism along two roughly linear, generally bimodal volcanic features: the High Lava Plains (HLP) of eastern Oregon and the eastern Snake River Plain (SRP) in southern Idaho. Both of these regions feature rhyolitic volcanism that has migrated in space and time; SRP volcanism has migrated to the northeast (roughly parallel to the absolute motion of the North American plate) since ~12 Ma and today is centered at Yellowstone Caldera, while HLP volcanism has migrated to the northwest (oblique to North American plate motion) over the same time interval. The western edge of the active volcano trace of the HLP is now in the region of Newberry Volcano and Three Sisters, the latter being an unusually active region of the Cascades. Both the HLP and SRP tracks have undergone

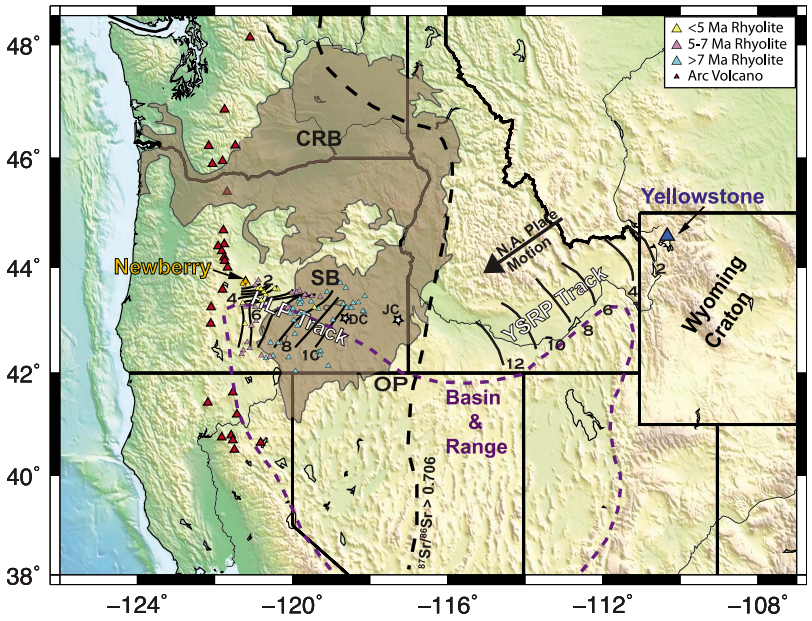

Figure 1. Map of the geologic and tectonic setting of the Pacific Northwest. Gray shaded region indicates the Steens flood basalts (SB) and Columbia River flood basalts (CRB). Red triangles indicate Cascades arc volcanoes. Young (<12 Ma) volcanism in the High Lava Plains (HLP) region is shown; blue, purple, and yellow triangles indicate the locations of HLP rhyolites, with colors indicating the age progression. Jordan Craters (JC) and Diamond Crater (DC) are shown with white stars. Black lines indicate age contours for the progressive rhyolitic volcanism in the HLP and Snake River Plain (SRP) volcanic tracks. The dashed purple line indicates the approximate northern extent of Basin & Range extension [e.g., *Wernicke et al.*, 1988], and the dashed black line indicates the Sr87/Sr86 = 0.706 line [e.g., *Leeman et al.*, 1992].

basaltic volcanism that is scattered in time and space, and there are Holocene basaltic eruptions throughout both regions (Figure 1).

[3] A wide variety of models have been proposed to explain the tectonomagmatic history of the PNW, including the location, timing, spatiotemporal progression, and geochemical and petrologic characteristics of the Steens/CRB, HLP, and SRP/Y volcanism. These models fall broadly into three categories (with some overlap): those that invoke a deep mantle plume as the major driver for the flood basalt eruptions and subsequent volcanism, those that explain volcanic trends mainly in terms of subduction-related processes, and those that invoke lithospheric processes as the main cause of volcanism. The Steens/CRB flood basalts are often interpreted as being the surface expression of a plume head impinging upon the base of the continental lithosphere [e.g., *Richards et al.*, 1989]; in this type of model, the Yellowstone/SRP trend is interpreted as reflecting the interaction of the plume tail with the moving North American plate above it [e.g., *Pierce and Morgan*, 1992; *Smith et al.*, 2009; *Obrebski et al.*, 2010]. Plume-type models have a bit more difficulty explaining the HLP volcanic trend, although in the context of these models the HLP may reflect the interaction of plume material with lithospheric basal topography or the subduction-related flow field [e.g, *Jordan et al.*, 2004; *Jordan*, 2005], or may be a consequence of an arm of the plume driving mantle flow along the strike of the HLP trend [e.g., *Camp and Ross*, 2004]. Models that emphasize the importance of lithospheric processes have also been proposed. For example, *Hales et al.* [2005] and *Camp and Hanan* [2008] discuss a lithospheric delamination model for the origin of the flood basalts, while *Cross and Pilger* [1978] emphasized the possible importance of lithospheric extension in producing PNW volcanism, particularly in eastern Oregon. Finally, several workers have espoused models that emphasize the importance of subduction processes in the post-20 Ma volcanic history of the PNW. This class of models includes work by *Carlson and Hart* [1987] that emphasized the role of the rollback and steepening of the Cascadia slab, as well as later studies by *Faccenna et al.* [2010], who proposed a series of mantle upwellings originating from the migrating tip of the Juan de Fuca slab at depth, and *Liu and Stegman* [2012], who proposed that the location

and timing of the Steens/CRB flood basalts was controlled by a tear in the subducting slab.

[4] Despite the long history of work on post-20 Ma tectonomagmatism of the PNW and the many papers that have been written on the subject, a consensus about what processes have controlled the timing and location of volcanic activity has not been forthcoming. In particular, whether or not a mantle plume is required to explain northwestern U.S. volcanism remains hotly debated [e.g., *Humphreys et al.*, 2000; *Christiansen et al.*, 2002; *Hooper et al.*, 2007; *Smith et al.*, 2009; *James et al.*, 2011; *Schmandt et al.*, 2012; *Fouch*, 2012]. Several recent large-scale projects in the PNW region have provided volumes of new data that can be exploited to shed light on the links between mantle processes and post-20 Ma tectonomagmatic activity. In this paper we discuss results from the recent High Lava Plains Project (www.dtm.ciw.edu/research/HLP), which brought together an interdisciplinary team of seismologists, geodynamicists, petrologists, geochemists, and structural geologists in order to understand the causes of continental intraplate magmatism in the HLP region. In particular, we focus on results from the petrology, geodynamical modeling, and broadband seismology components of the HLP project, and also discuss results from both our own and other research groups that leverage data from the seismic component of EarthScope's USArray Transportable Array (TA).

[5] The goal of this paper is to propose a conceptual model for mantle dynamics beneath the PNW over the past 20 Ma that adds the first-order observations gleaned from the HLP Project to the decades of study of the volcanic and tectonic history of the crust in this area. Our approach has been to start with basic "ingredients" for our model that are well known, and include the following: (1) the remnant Juan de Fuca slab is subducting beneath the PNW at a rate of 30 mm/yr in a NE direction [e.g., *Gripp and Gordon*, 2002], (2) the Juan de Fuca trench is currently rolling back at a rate of ~35 mm/yr [*Schellart et al.*, 2008] and a phase of relatively rapid rollback likely began at about ~20 Ma [e.g., *Atwater*, 1970; *Atwater and Stock*, 1998; see animation at http://emvc.geol.ucsb.edu/2_infopgs/IP4WNACal/bNEPacWNoAmer.html], (3) there is associated modest extension in the overriding plate [*Magill and Cox*, 1981; *Wells and Heller*, 1988], (4) the North American plate is moving over the underlying mantle in a SW direction (in a Pacific hot spot reference frame) [e.g., *Gripp and Gordon*, 2002], and (5) the Juan de Fuca plate is getting narrower as the Mendocino triple junction migrates to the north [e.g., *Atwater*, 1970]. This basic framework is combined with relatively well-constrained information about the location, timing, volume, and composition of post-20 Ma volcanism in the PNW; a review of current constraints on this volcanism is below. We then merge these constraints with new observations from the HLP Project and other recent work from petrologic estimates of the depths and temperatures of melting, seismological observations of mantle structure, and laboratory-based mantle dynamics experiments. The end result is a conceptual model that is consistent with the petrologic, seismic, and geodynamic observations highlighted in this paper, and can also explain the timing and patterns of PNW volcanism.

2. Overview of Geological Observations: Volcanic and Structural Constraints

[6] Here we present an overview of the most notable geologic events in the PNW from ~50 Ma to present, specifically structural and volcanic events, which represent important benchmarks for any model attempting to link mantle and crustal processes (Figure 2). Miocene to present volcanic activity in the PNW can be broadly described by three episodes of compositionally distinct volcanism: distributed calc-alkaline volcanism associated with subduction of the Farallon plate (~36–18 Ma), the flood basalt era (~16.6–10.5 Ma) and HLP/SRP volcanism (~12 Ma–present). By ~48 Ma arc volcanism had jumped westward from Idaho to near its current location in the Cascades when the Coast Range Basalt Province or Siletzia terrane was accreted to the western margin of North America [*Humphreys*, 2009; *Wells et al.*, 1998]. A peculiar aspect of PNW volcanism of this era is that calc-alkaline volcanism between ~37–18 Ma extended well to the east of the arc front as evidenced by the Clarno Formation of east-central Oregon [*Rogers and Novitsky-Evans*, 1977; *Gromme et al.*, 1986], the John Day Formation in northern Oregon [*Robinson et al.*, 1984], and in distributed, largely covered, volcanic centers in south-central Oregon and southwestern Idaho [*Norman and Leeman*, 1990; *Scarberry et al.*, 2010]. The character of volcanism changed dramatically at ~16.5 Ma when calc-alkalic volcanism was replaced by voluminous flood basalt volcanism that included eruptions of the Steens/CRB basalts. Eruption of the flood basalts initiated along north-south trending dikes near Steens Mountain in southeast Oregon and migrated north to the Chief Joseph and Monument dike swarms in northern Oregon [*Camp and Ross*, 2004].

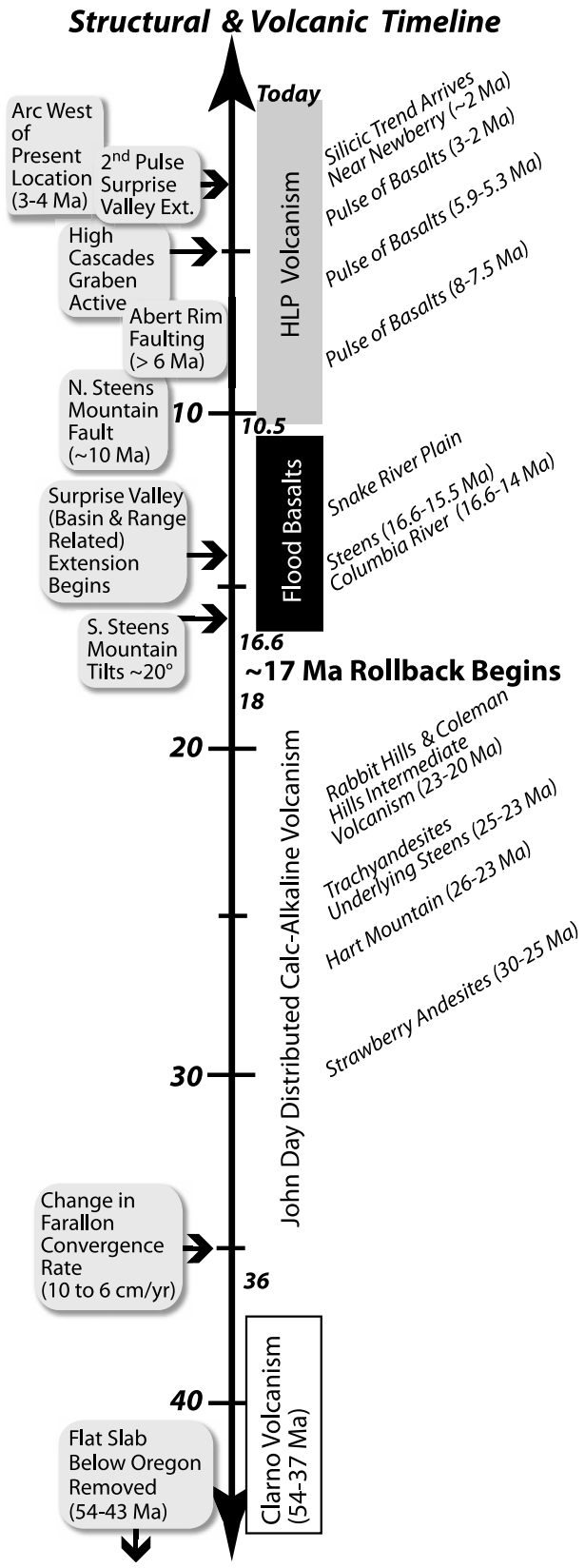

Figure 2. Timeline of the major structural and volcanic events in the Pacific Northwest over the past ~40 Ma that are relevant for our model, with a focus on the HLP region.

[7] The main phase of the Columbia River basalts continued for the next ~1.5 Ma with the Imnaha, Grande Ronde, and Picture Gorge Formations, covering much of northern and eastern Oregon as well as southern Washington with more than 250,000 km^3 of basalt [*Waters*, 1961; *Swanson et al.*, 1979; *Carlson and Hart*, 1987; *Tolan et al.*, 1989]. Coincident with flood basalt volcanism, large-volume silicic ignimbrite volcanism was widespread in southeastern Oregon surrounding the Owyhee plateau [*Brueseke et al.*, 2007]. By 12 Ma, the silicic volcanism reinitiated and began a spatiotemporal migration both to the NW along the Brothers Fault Zone in the HLP [*Jordan et al.*, 2004], and to the NE along the YSRP [*Pierce and Morgan*, 1992]. The present-day termination of these silicic volcanic tracks can be found at Yellowstone in the YSRP, and in the region between Newberry and Three Sisters volcanoes in the HLP. Around 10.5 Ma, effusive eruptions of primitive high-Al olivine tholeiite (HAOT) began in the HLP [*Hart et al.*, 1984]. This basaltic volcanism does not exhibit the same spatiotemporal migration as the silicic volcanism in the HLP, but three distinct pulses of basaltic volcanism are evident at 8–7.5, 5.9–5.3, and 3–2 Ma [*Jordan et al.*, 2004].

[8] The structural history of the PNW during the period of interest is characterized by the northwesterly migration of Basin and Range extension from central Nevada into Oregon starting in the late Oligocene [e.g., *Seedorf*, 1991; *Wernicke*, 1992]. Basin and Range extension and associated volcanism reached southern Oregon by ~22 Ma and continued to its northernmost terminus, the Brothers Fault Zone (BFZ), by ~10 Ma and its westernmost terminus, the High Cascade graben, by 5 Ma [e.g., *Scarberry et al.*, 2010, and references therein]. The WNW-trending BFZ is a broad region of small en echelon faults that coincides with the locus of HLP volcanism after 10 Ma, and may have acted as a transverse zone [e.g., *Rowley*, 1998]. Migration of Basin and Range extension is also evidenced by the timing of slip on larger regional escarpments, such as the Steens Mountain and Abert Rim faults (Figure 2). *Trench et al.* [2012] suggest that deformation in the BFZ coincided temporally with pulses of HLP basaltic volcanism, and argue that most individual BFZ faults accommodate dip-slip motion. Overall net extension in the HLP is thought to be relatively small compared to the central Basin and Range [e.g., *Wernicke*, 1992] with paleomagnetic estimates suggesting 17% net extension in WNW direction since 15 Ma [*Wells and Heller*, 1988] and

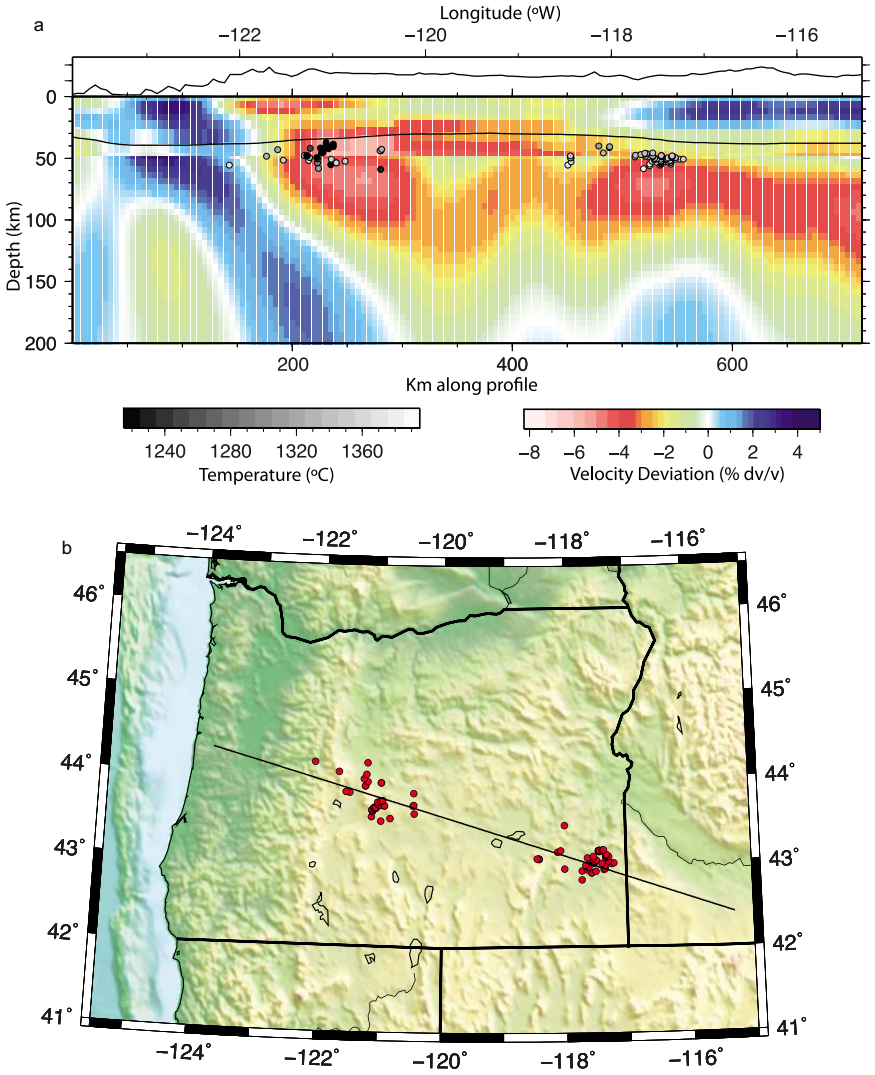

Figure 3. (a) Cross section along the strike of the HLP trend showing velocity structure of the crust and uppermost mantle along with the depths and temperatures of melting inferred from thermobarometry of HLP basalts, after *Till* [2011]. Background colors show deviation from a starting 1D velocity model obtained from the inversion of Rayleigh wave phase velocities derived from ambient noise cross-correlation (above 50 km depth) [*Hanson-Hedgecock et al.*, 2012] or event-based surface waves (below 50 km depth) [*Wagner et al.*, 2010]. Gray circles represent depths of inferred melt equilibration from young HLP basalts using the melting model of *Till et al.* [2012]; gray scale in circles represents the inferred temperature of melting. Line plot at top shows topography along the same cross section. (b) Map view showing the location of the samples used in the calculation of *Till* [2011] (red circles) and the location of the cross section (black line).

estimates based on crustal thickness suggesting 16% net extension since 10 Ma [*Eagar et al.*, 2011].

3. Petrologic Constraints

[9] Thermobarometric calculations for an extensive data set of young primitive basaltic lavas from across the HLP suggest that their minimum depth of equilibration with the asthenospheric mantle occurred at temperatures of ~1180–1380°C at 37–59 km depth [*Till*, 2011] (Figure 3). The basalts chosen for the calculations have high Mg#s (100 Mg/(Mg + Fe^T) at low SiO_2 (<52 wt.%), low phenocryst abundances, and trace element concentrations that indicate they are primitive mantle melts that have experienced a minimum of crystallization or alteration since they were removed from their source. The plagioclase and spinel lherzolite thermometer and barometer of *Till et al.* [2012] was used for the calculations because of its suitability for modeling melting of variably depleted and metasomatized mantle, such as that found below the PNW where there has been a long

history of subduction. All the samples are from lavas that erupted during the Quaternary in order to enable a comparison of their depths of melting to the geophysical observations, with the exception of samples erupted from unnamed vents in eastern Oregon and at South Sister [*Schmidt et al.*, 2008] and Mt. Bailey [*Barnes*, 1992] volcanoes in the Cascades arc, which have less well constrained ages but are likely younger than 10.5 Ma.

[10] Of the 111 samples with thermobarometric estimates, 23 exhibit petrologic and/or geochemical evidence for the involvement of H_2O during petrogenesis. All of these 23 basalts are from Newberry Volcano, which erupted both dry tholeiite and wet calc-alkaline basalts [*Donnelly Nolan and Grove*, 2009] during the last ~500 ka [*Jensen et al.*, 2009]. Olivine-plagioclase hygrometry on a representative subset of these 23 basalts indicates they contained ~4 wt.% H_2O prior to eruption [*Grove et al.*, 2009]. When this H_2O content is used with the correction for the effect of H_2O on the thermometer and barometer of *Till et al.* [2012], the average temperature and depth of origin for the 23 wet Newberry basalts are found to be 1213°C and 46 km, respectively. This is ~100–150°C cooler and 3–4 km deeper than the calculated temperature and depth of last mantle equilibration for these basalts at anhydrous conditions, as well as the dry basalts from Newberry included in this study. These results are consistent with the experimentally determined effect of H_2O on the conditions of mantle melting [e.g., *Gaetani and Grove*, 1998]. The pressures and temperatures discussed below and illustrated in Figure 3 include the H_2O-corrected values for the 23 wet Newberry basalts and the remaining 88 basaltic samples at anhydrous conditions.

[11] The shallowest depths of equilibration calculated for samples across the HLP (Figure 3) are immediately below the present-day geophysical Moho, as discussed in the following section, and occur at temperatures consistent with commonly assumed mantle potential temperatures and adiabatic gradients (or slightly lower temperatures for melts generated in the presence of small amounts of H_2O) [*Till*, 2011]. The petrologic constraints point toward a model where melting was driven by corner flow (i.e., upwelling in the asthenospheric mantle due to plate-driven flow processes) and to some extent toroidal flow around the southern edge of the Juan de Fuca and Gorda plates and/or upwelling due to lithospheric-scale extension, rather than melting triggered by the presence of deeper anomalously hot mantle as might be supplied by a mantle plume. In addition, the depths at which primitive Quaternary HLP basalts last equilibrated with the asthenospheric mantle imply that the geophysical Moho and the lithosphere-asthenosphere boundary were located at approximately the same depth for at least the last several million years in this region.

4. Seismologic Constraints

[12] Here we highlight results from the broadband seismology component of the HLP project that bear on the mantle dynamics of the PNW and also briefly discuss results that incorporate data from the larger region and make use of USArray TA data as well as other associated data sets. The HLP passive source experiment [*Carlson et al.*, 2005] consisted of 104 broadband seismographs deployed at 118 separate stations in the HLP province and surrounding locations. The HLP data set has been incorporated into a variety of analyses, including tomographic analysis of PNW mantle seismic velocities [*Roth et al.*, 2008; *Wagner et al.*, 2010; *Schmandt and Humphreys*, 2010; *James et al.*, 2011; *Hanson-Hedgecock et al.*, 2012], studies of mantle and crustal discontinuity structure from receiver functions [*Eagar et al.*, 2010, 2011], a study of mantle structure beneath the Kuriles from PP precursors [*Schmerr and Thomas*, 2011], and a study of the 19 February 2008 Oregon bolide event [*Walker et al.*, 2010]. Here we highlight results that are most relevant to understanding mantle dynamics beneath the PNW, principally results from shear wave splitting, surface wave dispersion analysis (including that derived from ambient noise), body and surface wave tomography, and receiver function analysis of crustal, lithospheric mantle, and mantle transition zone structure.

[13] Because of the link between mantle flow and the seismic anisotropy that results from the lattice preferred orientation (LPO) of upper mantle minerals, observations of upper mantle anisotropy provide some of the most direct constraints available on mantle flow [e.g., *Long and Becker*, 2010]. Early studies of shear wave splitting in the PNW [e.g., *Currie et al.*, 2004] were somewhat hampered by the sparse station coverage, but the advent of TA, HLP, and other data sets has improved this picture enormously. A map of single-station average SKS splitting parameters for stations throughout the PNW is shown in Figure 4 and includes measurements from the HLP experiment [*Long et al.*, 2009], from a catalog of uniform measurements

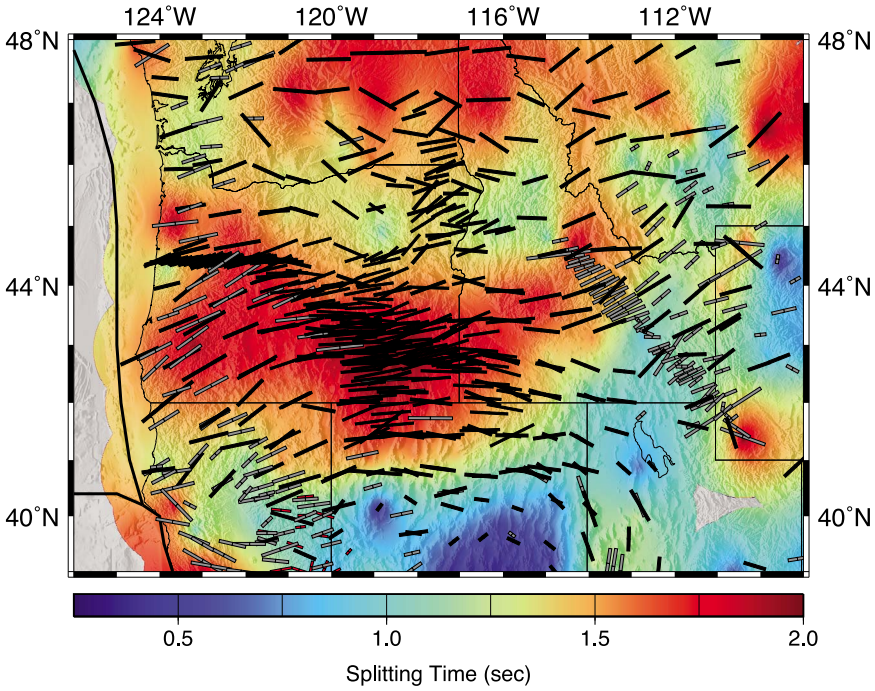

Figure 4. SKS splitting in the Pacific Northwest. Orientation and length of the bars indicate the fast polarization direction and delay time, respectively. Background colors indicate smoothed, contoured delay time values. Black bars are from the studies of *Fouch and West* [2008] and *Long et al.* [2009]. Gray bars indicate results from other authors, as compiled by *Eakin et al.* [2010].

for stations throughout the western U.S. [*Fouch and West*, 2008], and from other studies (as compiled by *Eakin et al.* [2010]). Beneath the HLP, delay times are very large (up to ~2.5 s) and fast directions are uniformly E-W. We have previously argued [*Long et al.*, 2009] that this is strong evidence for well-organized mantle flow in an E-W direction beneath the region. To the east of the HLP, in western Montana and eastern Idaho, there is a transition from E-W fast directions to NE-SW directions, which are roughly parallel to the absolute motion of the North American plate and are likely due to shear in the asthenosphere caused by plate motion [*Fouch and West*, 2008]. To the south of the HLP and the Mendocino Triple Junction, splitting patterns are more complex, leading to suggestions of flow around the southern edge of the Juan de Fuca slab [e.g., *Eakin et al.*, 2010], Juan de Fuca slab-driven toroidal flow throughout much of the western U.S. [e.g., *Zandt and Humphreys*, 2008; *Fouch and West*, 2008], and mantle downwelling associated with a well-documented minimum in delay times in central Nevada [*West et al.*, 2009].

[14] Constraints on upper mantle anisotropy complementary to those obtained from SKS analysis can be gleaned from surface wave dispersion analysis, which can place depth constraints on anisotropic structure, although the lateral resolution of surface wave models is much coarser than for SKS data sets. Models for azimuthal anisotropy for the PNW region derived from a combination of surface wave analysis and SKS analysis have been produced [e.g., *Yuan and Romanowicz*, 2010, *Lin et al.*, 2011] and these models indicate that anisotropy in the asthenospheric mantle probably makes the primary contribution to SKS splitting, at least beneath regions of thin lithosphere. Azimuthal anisotropy inferred from Rayleigh wave dispersion beneath the region surrounding the HLP [*Wagner et al.*, 2010] indicates strong anisotropy at periods of ~66 s, which are primarily sensitive to the depth range between ~50–150 km, with an average fast direction that is generally similar to those in the SKS data set. Finally, receiver function analysis of stations in the HLP and surrounding region did not yield evidence for azimuthal anisotropy in the crust [*Eagar et al.*, 2011], further cementing the notion that the bulk of the SKS splitting signal is derived from the mantle.

[15] Many different models to explain the large-scale pattern of seismic anisotropy in the western U.S. have been proposed, including those that invoke

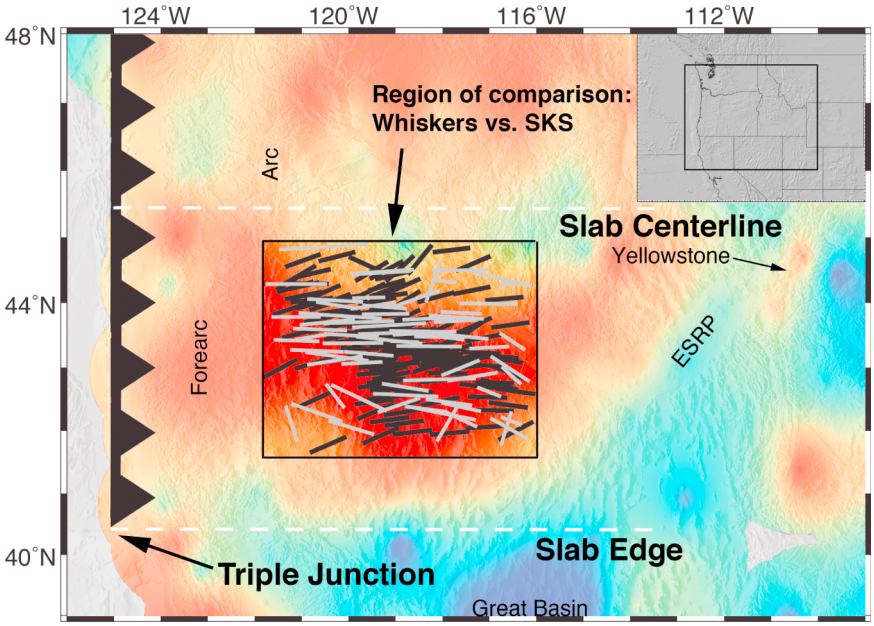

Figure 5. Schematic diagram and map of the comparison between geodynamical model predictions for mantle finite strain and observations of seismic anisotropy beneath the HLP. Background colors indicate smoothed and contoured shear wave splitting delay times for the western United States, as in Figure 4. The region of comparison beneath the HLP shows observed single-station average shear wave splitting fast directions as black bars (updated from *Long et al.* [2009]) along with observed whisker alignments (proxy for maximum finite strain) for the most "HLP-like" model run from the laboratory study of *Druken et al.* [2011]. Basic elements of the laboratory model geometry are overlain on the map, including the location of the trench (black line with hatches) and the location of the slab edge and slab centerline (dashed white lines).

toroidal flow around the Juan de Fuca slab edge [e.g., *Zandt and Humphreys*, 2008], a mantle downwelling beneath the Great Basin [*West et al.*, 2009], or a combination of density-driven flow and asthenospheric shear due to the overriding plate [e.g., *Silver and Holt*, 2002; *Becker et al.*, 2006]. We carried out comparisons between laboratory geodynamic modeling experiments, described in detail below, and the SKS splitting data sets, with a focus on explaining the consistent, strong anisotropy with an E-W fast symmetry axis beneath the HLP [*Druken et al.*, 2011]. We found that the rollback of the Cascadia slab likely results in focused mantle flow in the central part of the backarc parallel to the direction of rollback [*Druken et al.*, 2011]. A detailed comparison between finite strain directions measured from the laboratory flow models and the HLP SKS splitting data set (Figure 5) shows excellent agreement between the observations and the predictions for rollback-controlled flow. Our preferred model for explaining the pattern of upper mantle anisotropy in the PNW, therefore, is that mantle flow beneath the HLP is largely controlled by slab rollback, while further to the east in the eastern part of the Snake River Plain and beneath Yellowstone, the effect of rollback dies off, allowing a transition to North American plate driven flow. This view of mantle flow is generally consistent with the toroidal flow model proposed by *Zandt and Humphreys* [2008]. Such a model explains the large-scale pattern of SKS splitting observed in the western U.S., but there are likely local perturbations to this large-scale flow, such as the proposed mantle downwelling beneath the Great Basin [*West et al.*, 2009].

[16] The structure of the transition zone (TZ) can also shed light on mantle dynamics, because the exact position of the major discontinuities (nominally at 410 and 660 km depth) will depend on conditions such as temperature [e.g., *Bina and Helffrich*, 1994] and water content [e.g., *Smyth and Jacobsen*, 2006]. Transition zone discontinuity topography thus can reflect thermal buoyancy-driven processes such as upwelling and downwelling [e.g., *Niu et al.*, 2005; *Deuss*, 2007; *Schmerr and Thomas*, 2011; *Schmandt et al.*, 2012] and can be interpreted, sometimes in combination with seismic anisotropy observations [e.g., *Long et al.*, 2010], in terms of mantle dynamics. The availability of TA data in the western U.S. has enabled several recent studies of the detailed TZ discontinuity structure in our study region [e.g., *Cao and Levander*, 2010; *Eagar*

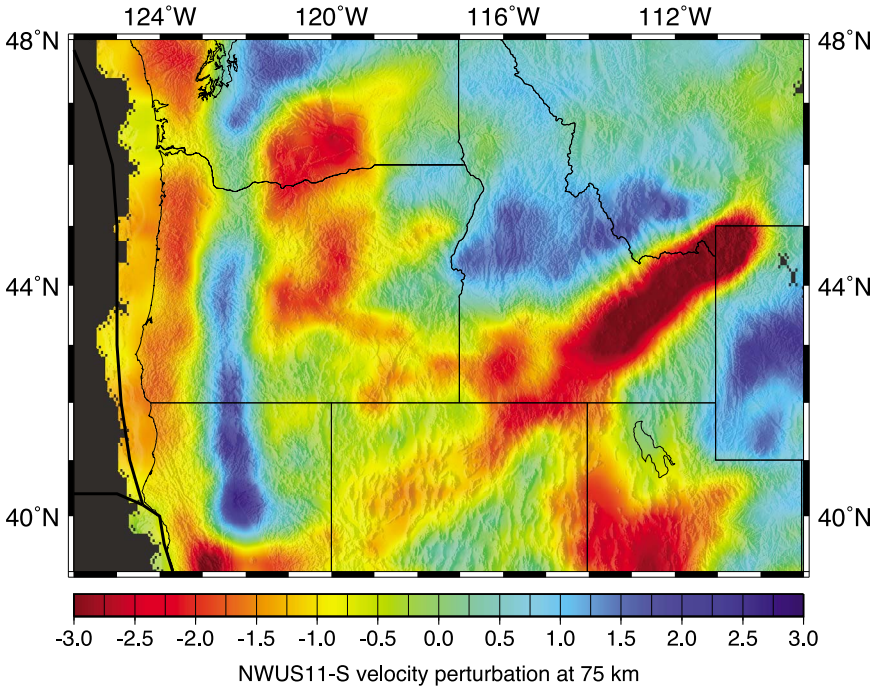

Figure 6. Map view of S wave speed perturbations at 75 km depth, from the tomographic model of *James et al.* [2011]. Background colors represent relative wave speed perturbations (in percent).

et al., 2010; *Schmandt et al.*, 2012]. Studies that have incorporated data from the HLP deployment [*Eagar et al.*, 2010; *Schmandt et al.*, 2012] have identified some evidence for locally cooler temperatures associated with the penetration of the Juan de Fuca slab into the transition zone, but along-strike variations are observed which are consistent with slab fragmentation at transition zone depths. *Eagar et al.* [2010] argued that there is no evidence for significant transition zone thinning directly beneath the HLP, as would be associated with a mantle plume. However, *Schmandt et al.* [2012] finds evidence for hotter temperatures in the transition zone beneath the Yellowstone hot spot. In particular, *Schmandt et al.* [2012] identified an upwards deflection by ∼12–18 km of the 660 km discontinuity beneath Yellowstone and argued that this is consistent with a plume-like upwelling across the 660.

[17] Constraints on the isotropic velocity structure of the mantle beneath the PNW are also important for understanding the mantle dynamics over the past 20 Ma, because they can shed light on the location and shape of the slab at depth, as well as delineate any slow mantle features that may correspond to a mantle plume or other type of focused upwelling. Several groups have produced tomographic images of the entire western U.S., with a large number of published models derived from body waves [e.g., *Sigloch et al.*, 2008; *Burdick et al.*, 2008, 2012; *Xue and Allen*, 2010; *Obrebski et al.*, 2010; *Schmandt and Humphreys*, 2010], models derived from surface waves and/or ambient noise [e.g., *Moschetti et al.*, 2007; *Yang and Ritzwoller*, 2008; *Gao et al.*, 2011], or models that combine body and surface waves [e.g., *Bedle and van der Lee*, 2009; *Obrebski et al.*, 2011]. Here we mostly discuss the results produced from the HLP Project [*Warren et al.*, 2008; *Roth et al.*, 2008; *West et al.*, 2009; *Wagner et al.*, 2010; *James et al.*, 2011; *Hanson-Hedgecock et al.*, 2012], with a focus on the HLP and Yellowstone/Snake River Plain regions. However, we emphasize that there are many first-order similarities among the tomographic models produced by different groups [e.g., *Pavlis et al.*, 2012; *Becker*, 2012], and many of the features we describe here are also found in other models, although the implications of many of these features remain under debate.

[18] *James et al.* [2011] document P and S wave tomography models produced using a combination of the TA and HLP broadband data sets. Here we summarize the features of their tomographic models that are most salient for our understanding of mantle dynamics; a map view of the relative S wave

speed perturbations at a depth of 75 km is shown in Figure 6. The downgoing Juan de Fuca slab is well-imaged in the body wave models as a semi-continuous, higher-velocity anomaly down to the deep upper mantle (>300 km) with a southern edge extending along the NE-SW direction of plate motion passing from the Mendocino triple junction in California across northernmost Nevada. The most striking feature of the upper mantle beneath the region is the very strong lower-velocity anomaly beneath the entire eastern SRP (Figure 6). In contrast, wave speeds beneath the HLP and Newberry Volcano are low, but not as low as beneath the SRP and the lower velocity material is confined only to the shallowest mantle.

[19] The body wave tomography further reveals that a sub-horizontal branch of the old Farallon plate, orphaned from the descending plate by the northward migration of the Mendocino triple junction, resides in the mantle transition zone (400–600 km) directly beneath the SRP/Y track. Its truncated northern edge is parallel to the northwestern margin of the hot spot track itself and marks the southern edge of a prominent slab gap anomaly that was first noted by *Sigloch et al.* [2008]. As with other western U.S. tomography, evidence for a continuous lower-velocity feature beneath Yellowstone in the models of *James et al.* [2011] that corresponds to what might be expected for a classical plume conduit is ambiguous, although there is a relatively weak region of lower velocities that extend down to the transition zone in a warped, sheet-like structure spatially connected with the prominent slab gap anomaly in the transition zone on the northwest edge of the SRP/Yellowstone province. *James et al.* [2011] interpret these various features as supporting a model that involves a sheet-like upwelling from the transition zone along the length of the SRP, and note the similarities with geodynamic models that predict upward flow around the edge and/or tip of a retreating slab [*Faccenna et al.*, 2010]. While the seismic images also reveal a broad low velocity anomaly in the mid-mantle (uppermost lower mantle) beneath Yellowstone, the sub-horizontal stagnating slab may block vertical ascent from the deeper mantle.

[20] Complementary constraints on upper mantle velocities have been obtained from surface wave tomography; surface wave models have the advantage of being able to resolve shallow mantle features well and can also provide constraints on absolute velocities. A surface wave study by *Warren et al.* [2008] used data from the first phase of the HLP broadband experiment and found support for relatively low uppermost mantle S velocities (∼4.1 km/sec) beneath the HLP, with the lowest velocities coinciding geographically with regions of Holocene basaltic volcanism. The regionally more extensive 3D isotropic model of *Wagner et al.* [2010], which used the entire HLP data set, also identified relatively low S velocities beneath the HLP and Newberry Volcano and argued that these are consistent with a thin lithosphere; indeed, there may be little or no mantle lithosphere beneath the region. A vertical cross-section through this model along the strike of the HLP track (Figure 3) shows a clearly imaged Juan de Fuca slab along with a somewhat intermittent low velocity anomaly in the uppermost mantle (∼50–100 km depth). *Wagner et al.* [2010] also found a striking low-velocity anomaly beneath the eastern SRP, with velocities 3% lower than the reference model persisting down to a depth of ∼100 km and the anomaly deepening somewhat (down to at least 175 km) beneath Yellowstone.

[21] The high-resolution tomographic models that have been produced using TA and HLP data allow for the investigation of the detailed structure of the subducting Juan de Fuca slab, and specifically the degree of slab fragmentation at depth. Several different studies have pointed out that the high velocity anomaly in the models that corresponds to the subducting slab does not appear to be continuous with depth or along strike [e.g., *Roth et al.*, 2008; *Burdick et al.*, 2008; *Schmandt and Humphreys*, 2010; *Tian et al.*, 2011; *Obrebski et al.*, 2011]. In particular, several of these workers have noted that the slab is not imaged well beneath central Oregon at depths beneath ∼150–200 km, and have argued for the fragmentation of the slab in the upper mantle. However, *Roth et al.* [2008] argued that this apparent fragmentation may actually reflect an imaging artifact due to the presence of a prominent low velocity anomaly in the adjacent mantle wedge. There is general consensus that the slab is likely fragmented deeper in the mantle, at transition zone and uppermost lowermantle depths. *Sigloch* [2011] and *James et al.* [2011], among others, have argued for significant fragmentation of the slab in the transition zone.

[22] Finally, constraints on crustal structure, in particular crustal thickness values, are relevant for our model since a comparison between the depth of melting inferred from petrology and Moho depths inferred from seismology can yield insight into the mantle processes that are controlling the generation, transport, and extraction of melt. Constraints

on crustal structure beneath the HLP and the surrounding region have been obtained from two complementary techniques applied to broadband data: receiver function (RF) analysis [*Eagar et al.*, 2011], which yields information on both the thickness and bulk Vp/Vs ratio of the crust, and ambient noise tomography [*Hanson-Hedgecock et al.*, 2012], which excels at resolving lateral variations in shallow structure. Crustal thickness values obtained from H-κ stacking of receiver functions [*Eagar et al.*, 2011] show generally relatively thin crust (~31 km) beneath the HLP and northern Great Basin compared to the adjacent regions of the Cascades and Owyhee Plateau. A remarkable correlation has emerged between the depth of melting for young basalts in the HLP inferred from a petrologic model [*Till*, 2011] and Moho depths and isotropic velocities estimated from broadband seismology [*Wagner et al.*, 2010; *Eagar et al.*, 2011; *Hanson-Hedgecock et al.*, 2012], as discussed above and shown in Figure 3. This correlation supports the idea that there is little, if any, mantle lithosphere beneath the HLP, and that melt equilibration occurs at shallow depths near the base of the crust.

5. Geodynamic Modeling Experiments

[23] Geodynamic models have long been employed to investigate melt production in subduction zones [e.g., *Spiegelman and McKenzie*, 1987; *McCulloch and Gamble*, 1991; *Hebert et al.*, 2009]. Decompression melting is related to upwelling rates; mantle upwelling has been shown to result from the initiation of subduction [*Faccenna et al.*, 2010], differences in the style of slab sinking [*Kincaid and Sacks*, 1997; *Kincaid and Hall*, 2003; *Kincaid and Griffiths*, 2004], segmentation or breakup of the slab [*Liu and Stegman*, 2011, 2012], and extension within the overriding plate [*Ribe*, 1989; *Conder et al.*, 2002; *Kincaid and Hall*, 2003; *Hall et al.*, 2012]. Subduction-driven upwelling in the PNW has been proposed and modeled to explain specific features of volcanic surface expressions [*Faccenna et al.*, 2010; *Liu and Stegman*, 2012].

[24] Here we report idealized laboratory experiments designed to examine the combined effects of trench migration, slab steepening, and modest upper plate extension on the mantle flow field in the PNW. The plate-driven flow fields are examined using the kinematic subduction model setup of *Druken et al.* [2011] and *Kincaid and Griffiths* [2003, 2004], which uses glucose syrup, a rigid fiberglass plate, and mylar sheeting to model the upper mantle, subducting plate, and overriding plate extension respectively. Plate rates were scaled to match those of the southern half of the Cascadia subduction system (as described in *Druken et al.* [2011]) and the flow fields were quantified using particle tracking techniques [e.g., *Funiciello et al.*, 2006]. A key finding of these experiments is that simple plate forcings can give rise to complex and evolving 3-D flow fields.

[25] During the early stages of subduction (Figures 7a–7b), the downdip sinking of the plate naturally induces an upwelling [e.g., *Faccenna et al.*, 2010], though the amount is small compared with the large pulse that follows the subsequent initiation of rollback and extension (Figures 7c–7d). Vertical velocities within the wedge are shown to peak rapidly within 3 Ma of rollback and extension initiation but vary spatially from the center of the slab toward the edge. Upwelling reaches an approximate steady state after ~20–25 Ma (Figures 7e–7f) but mantle flow is still continually focused toward the center by rollback and stretched E-W by the combination of slab-driven shear flow (i.e., poloidal) and extension. A front of micro-bubbles within the fluid (Figure 7, red line) highlights this evolution. The front originates off the slab edge with a concave shape but toroidal and poloidal/extensional motions push and stretch the front with time.

[26] The flow fields show that this north-south temporal trend is a consequence of the combination of slab sinking motions (i.e., downdip and rollback) and extension of the overriding plate. This is evident in the upwelling patterns as well as the thermal evolution beneath the overriding plate (Figure 8a). Temperature measurements along the "trench" after ~20 Ma of rollback and extension display a dramatic temperature increase toward the slab centerline, consistent with slab surface measurements that show the same pattern [*Kincaid and Griffiths*, 2003, 2004]. Equivalent scaled mantle anomalies are almost on the order of hot spot temperatures [*Courtier et al.*, 2007; *Herzberg and Gazel*, 2009].

[27] For comparison, rollback motion without extension (blue triangles) shows no distinct warming, nor a north-south variation. Rollback alone tends to draw material horizontally from around the slab edges with very little vertical motion [*Kincaid and Griffiths*, 2004]. Combined with extension, however, the flow pattern adjusts to draw both laterally as well as from depth. We note that the amount of upper plate extension in our experiments is relatively modest and is consistent with geologic estimates for the amount of extension

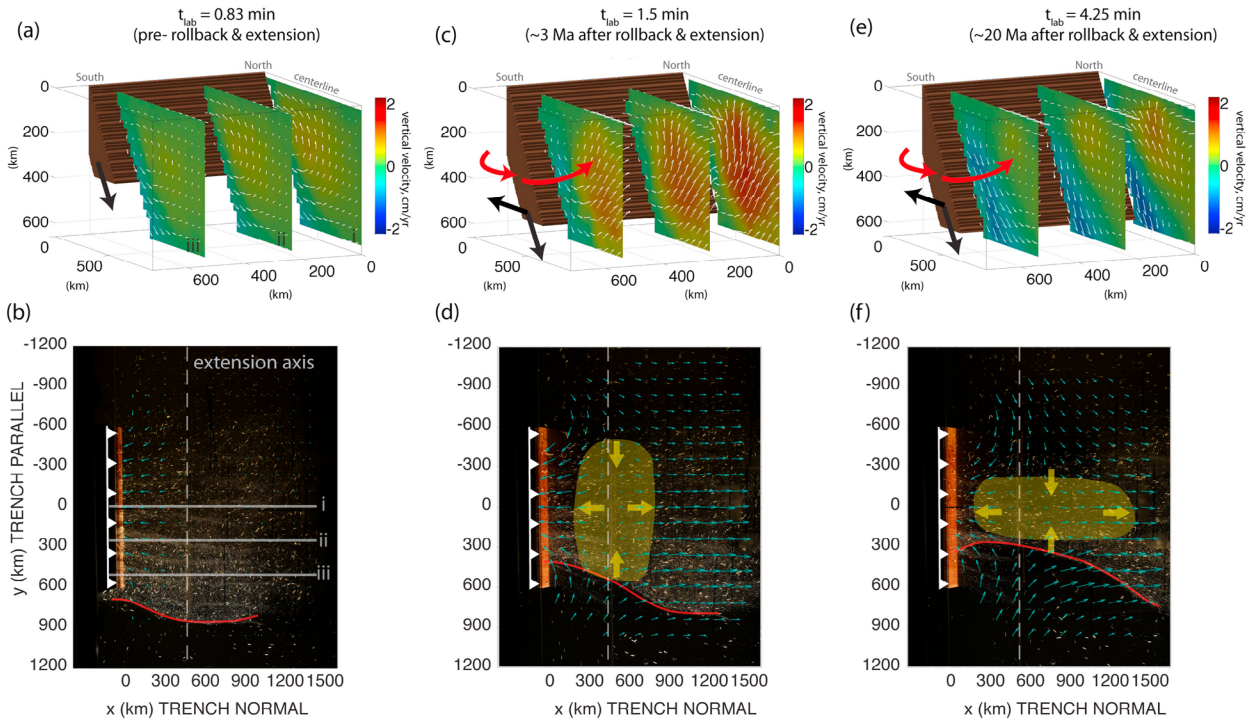

Figure 7. The time evolution of the slab-induced flow field from vertical and map-view perspectives for the laboratory model of *Druken et al.* [2011]. Scaled mantle rates for subduction, rollback, and the extension of the overriding plate are approximately 4.4 cm/yr, 2.6 cm/yr, and ±1.3 cm/yr, respectively, and correspond to Experiment 34 of *Druken et al.* [2011]. Vertical cross-sections are colored by upwelling magnitude. (a–b) The slab initially subducts with downdip sinking motion only, inducing small amounts of upwelling relatively constant along trench. (c–d) Initiation of slab rollback and extension of the overriding plate produces a large pulse of upwelling focused toward the slab centerline. Extensional motion generates a vertical component of motion along trench but rollback-induced, toroidal motion reduces this effect near the slab edges. (e–f) As subduction continues, upwelling decreases until the flow field reaches an approximate steady state phase. Shaded yellow areas and red line illustrate the continued extension and focusing of the plate motions with time. Flow fields were produced from particle tracking techniques and are fixed relative to the motion of the trench. Black and red arrows illustrate slab sinking velocities and rollback-induced toroidal motion, respectively.

beneath the HLP [*Magill and Cox*, 1981; *Wells and Heller*, 1988].

[28] With respect to the PNW (and discussed in more detail in section 6), the position of maximum mantle upflow relative to the slab edge is consistent with the decreasing volumes of volcanism moving south from the CRB through Steens to the smaller volumes of contemporaneous volcanism in northern Nevada. The decreased, but more focused, upwelling that follows the larger pulse may also explain the lower volume HLP basalts. Petrologic constraints, in particular, are in strong agreement with a plate-driven upwelling that is stronger beneath HLP than further south. Temperature measurements within the central wedge, however, not only increase with time (Figure 8a) but this increase also migrates trench-ward as well (Figure 8b). This provides mechanisms for both the basaltic and time-progressive rhyolitic volcanism in the HLP trend. The thermal signal (recorded at depths equivalent to ~50–75 km) from the plate-driven upwelling first begins near the extension axis (dark blue curve, Figure 8b) and then migrates at a rate of ~26 km/Ma toward the trench (light blue curve). Despite the simplified geometry and plate motions used in our laboratory model, this thermal progression is within the 2–33 km/Ma range suggested by *Jordan et al.* [2004] for HLP rhyolites.

[29] The geodynamic experiments, although simplified, highlight fundamental variations in mantle flow that result from the combination of plate motions similar those found in the PNW. If a plume

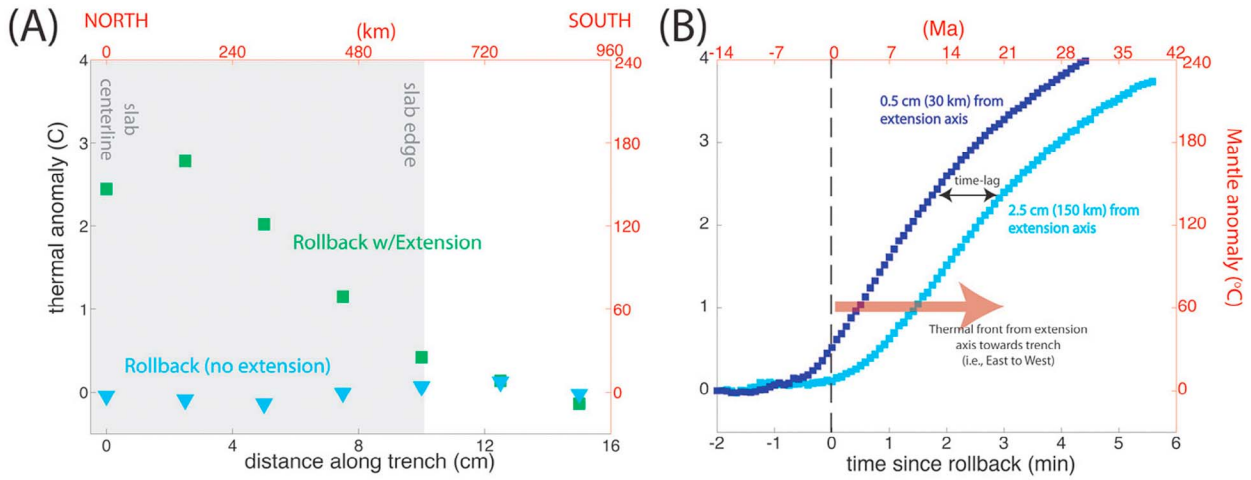

Figure 8. (a) Thermal anomalies below the overriding plate along the trench (centerline toward edge) for the laboratory model of *Druken et al.* [2011]. Measurements were taken at scaled mantle distances of ~50–75 km depth and ~120 km away from the trench. Model with rollback and extensional motions produce a significantly larger thermal signal than rollback alone, which varies north–south along trench. (b) Thermal anomalies at two positions demonstrating the spatiotemporal progression of the temperature increases. The temperature profile at a position corresponding to ~30 km from the extension axis is shown in dark blue; the corresponding temperature profile for a position ~150 km from the extension axis is shown in light blue. Thermal anomalies within the laboratory model were scaled to mantle values as in *Kincaid and Griffiths* [2004].

is present within the region, it too will be subjected to the surrounding plate-driven circulation. Geodynamic models of plume-slab interaction [*Kincaid et al.*, 2009; *Druken et al.*, 2009] show that the motion of plumes rising near subduction zones is dominated by slab-driven flow, with plumes generally acting as passive thermal anomalies and not active drivers of mantle flow. In a tectonic setting such as the PNW, therefore, plate-driven models are important to consider regardless of possible plume involvement.

6. A Conceptual Model for Mantle Dynamics Beneath the PNW

[30] Given the constraints from the petrology, geodynamics, and broadband seismology components of the HLP project, along with constraints on plate kinematics and the timing and location of volcanism, we have developed a conceptual model for PNW mantle dynamics and the links between mantle processes and surface tectonomagmatism. In particular, our goal has been to propose a model that is consistent with four important and robust observations that have emerged from recent studies. First, the robust constraints on seismic anisotropy argue for well-organized contemporary mantle flow beneath the HLP in an E-W direction, and comparisons with geodynamic models argue strongly for slab rollback-controlled flow beneath the HLP, with a transition to plate motion-controlled asthenospheric shear to the east. Second, body and surface wave tomography argue for very low uppermost mantle velocities beneath both the SRP and the HLP, with the SRP low-velocity anomaly being particularly pronounced. Body wave tomography is also able to resolve the fragmentation of the Juan de Fuca slab in the transition zone and uppermost lower mantle. Third, the geodynamic modeling studies indicate that the initiation of slab rollback at ~20 Ma was likely associated with a large pulse of mantle upwelling that increased in magnitude from the southern edge of the slab in northern Nevada northward past Steens to a maximum in the region of the dike swarms for the main volume of the CRB eruptions. Continued broad upwelling beneath the HLP enhanced by rollback-controlled mantle flow followed the flood basalt era. Fourth, the modern lithosphere beneath the HLP is thin, and petrologic models indicate that HLP basalts are produced by shallow decompression melting near the base of the seismically imaged crust.

[31] These constraints are synthesized into the following model, which is shown in schematic cartoon form in Figure 9. Constraints from plate tectonic reconstructions [e.g., *Atwater*, 1970; *Atwater and Stock*, 1998] and the broad distribution of calc-alkaline volcanism across the PNW between 18

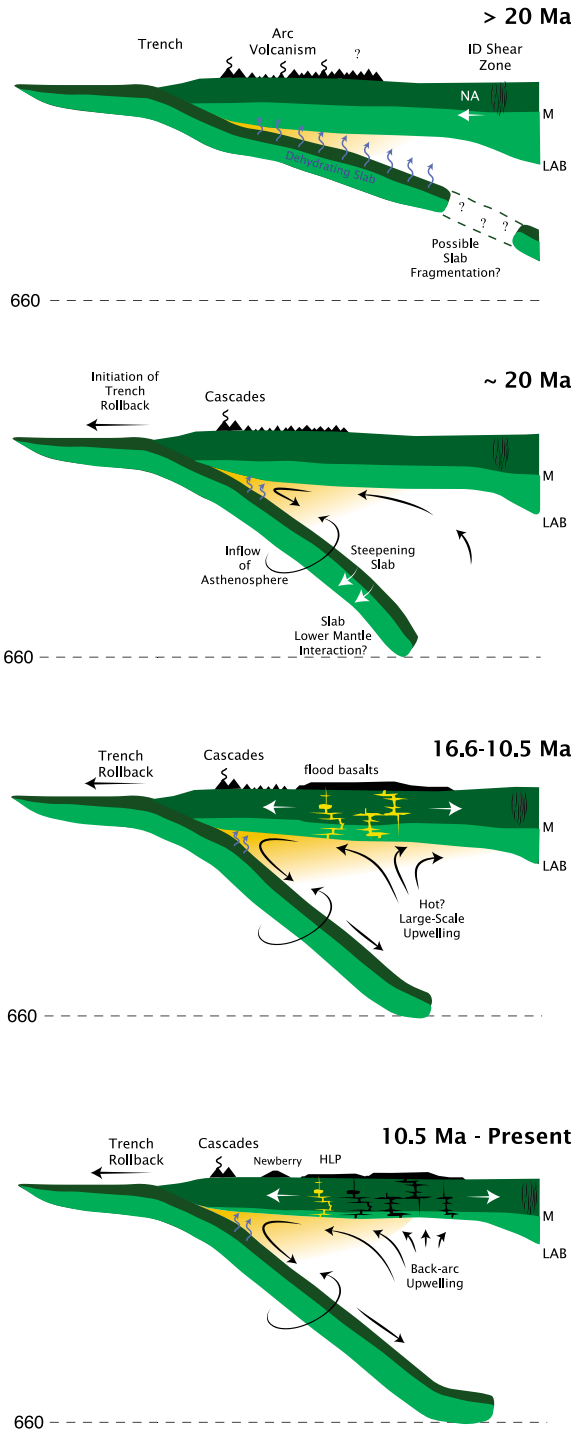

Figure 9. Schematic cartoon sketch of the main features of our model at four time periods: pre-18 Ma, ~18 Ma (initiation of rollback), 16.5–10.5 Ma (flood basalt era), and 10.5 Ma-present (HLP/SRP era). Because of the uncertainty surrounding the origin of the upwelling responsible for Yellowstone/SRP volcanism, the cartoon focuses on the flood basalt eruptions and subsequent HLP volcanism.

and 35 Ma suggest that prior to ~20 Ma, the Juan de Fuca plate was subducting with a fairly shallow dip. Plate tectonic reconstructions [e.g., *Atwater*, 1970; *Atwater and Stock*, 1998] indicate that a phase of slab rollback (and presumably steepening as well) began around ~20 Ma. This change in subduction motions, particularly the initiation (or acceleration) of rollback, may have been the result of the decreasing trench width along the western U.S. margin [*Schellart et al.*, 2010]. We note that while there is a noticeable phase of slab rollback beginning around ~20 Ma in the reconstruction of *Atwater and Stock* [1998], there are some differences among different plate motion models about the timing and velocity of slab rollback and upper plate extension in the PNW, and some studies argue that the slab has been rolling back since at least the early Miocene [e.g., *Müller et al.*, 2008]. While our conceptual model invokes a phase of increased rollback and upper plate extension, our framework can accommodate this level of uncertainty in its exact timing, particularly given the uncertainties about the time scales needed to generate and extract large volumes of melt from the upper mantle.

[32] We propose that the phase of rapid slab rollback and steepening that initiated at ~20 Ma enabled a large pulse of mantle upwelling (Figure 9), as suggested by our geodynamic modeling results. This upwelling facilitated rapid thinning (both convective and advective) of the overriding lithosphere as well as extensive mantle melting, which represents the source of the Steens and Columbia River flood basalts. The geodynamic experiments show that mantle upwelling would have been limited near the southern slab margin, explaining the rapid reduction in magmatic volumes moving south from Steens Mountain to the contemporaneous volcanic centers in the Northern Nevada rift. The upwelling induced by slab rollback would be most prominent near the center of the subducting plate, providing a ready explanation for the eruption of the largest volume of flood basalts near the Washington-Oregon border (rather than at the assumed impact point of a putative plume near the Oregon-Nevada border). Although the extensive mantle melting was a direct consequence of slab rollback and extension, the surface expression of the flood basalts was likely controlled by preexisting structures in the lithosphere, with the feeder dikes of the St. Joseph dike swarm parallel to the edge of the North American craton (Figure 1).

[33] As the subduction system continued to evolve post-17 Ma (Figure 9), we envision that the upper mantle beneath the HLP experienced a

reorganization of the prevailing flow field to the rollback-controlled flow field that we infer today. In our geodynamic models, continuing rollback is associated with ongoing upwelling and elevated uppermost mantle temperatures beneath the central part of the far backarc, corresponding to the HLP. We suggest that the rollback-controlled flow field, with a component of toroidal flow around the southern edge of the Juan de Fuca slab, became well established in the few million years following the initiation of trench migration and the large pulse of upwelling that resulted in the Steens/CRB volcanism. Continued upwelling beneath the HLP, in combination with ongoing modest extension of the upper plate lithosphere, facilitated ongoing convective and advective thinning of the lithosphere beneath the HLP. The combination of thinned lithosphere and continued upwelling allows for the generation of relatively small volumes of mantle melt at shallow depths beneath the HLP, consistent with petrologic investigations of young HLP basalts (Figure 3). The rollback-controlled flow field results in dominantly E-W mantle flow beneath the HLP (Figures 4 and 5), consistent with the seismic anisotropy results, and a critical component of ongoing mantle upwelling (Figure 7) to produce shallow mantle melting and related volcanism in the HLP over the past 10.5 Ma. The westward migration of HLP volcanism then is primarily a reflection of the plate-induced flow field, which causes the center of rollback-associated upwelling to move westward. The concentration of volcanism along the HLP may be controlled (at least in part) by lithospheric processes. The Brothers Fault Zone, for example, may serve as a means to ease magma flow through the crust. Poisson's ratios for the crust [*Eagar et al.*, 2011] and crustal conductivities [*Patro and Egbert*, 2008] show high values throughout eastern Oregon, suggesting of the presence of melt throughout this area, but the Poisson's ratios and conductivity directly beneath the HLP are somewhat reduced, perhaps reflecting that in this area, crustal melts have managed to erupt [*Eagar et al.*, 2011].

[34] This model is consistent with petrologic, geodynamic, and seismologic observations beneath the HLP, but it does not provide an obvious explanation for the Y/SRP trend to the east. One possibility is the scenario discussed by *James et al.* [2011] and summarized above, which invokes mantle upwelling around the tip and edge of the sinking remnant slab driven by slab rollback. Alternatively, the deep mantle plume model has been espoused by many workers [e.g., *Richards et al.*, 1989; *Camp and Hanan*, 2008; *Obrebski et al.*, 2010]. However, modeling experiments of *Druken et al.* [2010] show that slab-driven flow strongly influences active upwelling of plumes over large distances (up to ~2000 km). This suggests that if there were a deep mantle plume beneath Yellowstone, the plume material would effectively act as a passive tracer in the rollback-controlled flow field and plume material would be drawn into the mantle beneath the HLP and distributed throughout the HLP region. There is, however, no unambiguous geochemical or petrologic evidence for a deep mantle plume signature in HLP rocks [*Carlson*, 1984; *Carlson and Hart*, 1987; *Graham et al.*, 2009; *Till et al.*, 2012].

[35] There is a plausible alternative scenario in which mantle dynamics beneath the PNW are largely controlled by subduction-related processes. In this scenario, the initiation of the pulse of slab rollback at ~17 Ma (and possibly the fragmentation of the Farallon slab) facilitated the upward transport of a parcel of buoyant upwelling mantle that constitutes the mantle source of the SRP/Y magmas. The exact nature of this buoyant upwelling that constitutes the source of the SRP/Y volcanism remains unresolved, and a detailed discussion of possible models is beyond the scope of this paper. Regardless of what process is responsible for the mantle upwelling beneath the SRP/Y trend, however, our conceptual model provides a plausible framework for explaining the broad features of post-17 Ma volcanism, including the flood basalts, the HLP, and the SRP, within the context of subduction-related processes.

7. Discussion and Summary

[36] Our conceptual model for PNW mantle dynamics has been informed by constraints from seismology, petrology, and geodynamical modeling experiments. We emphasize that our laboratory experiments make a large number of simplifying assumptions, including the use of a completely rigid, kinematically defined slab, simplified plate motions, and a simple viscosity structure. Despite this, however, our experiments produce a spatiotemporal complexity in mantle flow that, to first order, matches the available observations (from volcanic history, seismic anisotropy, seismic tomography, petrologic data, etc.). Of course, our simplified experimental setup cannot possibly capture all of the spatiotemporal complexity of the PNW subduction system. However, the fundamental responses of plate-driven flow found in our experiments provide an important backdrop for future

modeling studies, which can continue to add complexity. We further note that while the evolution of the slab in our experiments is imposed kinematically, it is done so in a way that is consistent with previous fully dynamic 3D subduction experiments [e.g., *Kincaid and Olson*, 1987; *Griffiths et al.*, 1995], in which slabs heat up and weaken as they descend, leading to more efficient bending at depth and an increase in dip angle with time.

[37] Our model emphasizes the importance of subduction-related processes such as slab rollback, extension, and steepening in controlling the mantle dynamics and surface volcanism of the PNW over the past ~17 Ma. This view contrasts with other models of the region, particularly those that invoke a classical mantle plume as the cause of the Steens/CRB flood basalts [e.g., *Richards et al.*, 1989; *Takahahshi et al.*, 1998; *Wolff et al.*, 2008; *Camp and Hanan*, 2008; *Obrebski et al.*, 2010] and subsequent volcanism in the SRP [e.g., *Pierce and Morgan*, 1992; *Smith et al.*, 2009] and HLP [e.g., *Camp and Ross*, 2004; *Jordan*, 2005]. Our model does, however, share some similarities with other recent models that have explored non-plume explanations for recent PNW volcanism. For example, *Faccenna et al.* [2010] recently proposed a model that invokes a series of mantle upwellings from the tip and around the side of the migrating Juan de Fuca slab at depth to explain the timing of PNW volcanism. Recent work by *Liu and Stegman* [2012] has suggested that the CRB flood basalts may be a consequence of a propagating rupture in the Farallon slab at depth.

[38] Our model differs in its details from the models of *Faccenna et al.* [2010] and *Liu and Stegman* [2012], and it is worth examining these differences and the predictions made by each of these models about present-day mantle flow. The study of *Liu and Stegman* [2012] proposes that the Steens/CRB flood basalt episode was a result of rapid mantle upwelling through a tear in the Farallon slab at depth. While this model is conceptually similar to ours in that it invokes subduction-related processes as the source of the Steens/CRB mantle upwelling, a major difference is that we do not invoke a slab tear and instead predict a pulse of upwelling due to the rollback of a rigid, coherent slab. Our conceptual model is more similar to that proposed by *Faccenna et al.* [2010], which also invokes 3D mantle flow at slab edges as a mechanism for mantle upwelling and surface volcanism and applies this concept to western North America, although the details are slightly different. Specifically, our model provides a ready explanation for the time-progressive HLP rhyolite track, as well as the timing and expression of the flood basalts with the observed spatial variations in volcanic production. While the details of our model are different from those proposed by *Faccenna et al.* [2010] and *Liu and Stegman* [2012], they share a conceptual similarity in that they invoke subduction-related processes, rather than a mantle plume, as the primary control on mantle dynamics, melting, and surface volcanism in the PNW. The predictions made by the models of *Faccenna et al.* [2010] and *Liu and Stegman* [2012] about the present-day mantle flow field and the resulting patterns of seismic anisotropy have not yet been examined in great detail, but we suggest that the striking pattern of anisotropy observed beneath the PNW [*Fouch and West*, 2008; *Long et al.*, 2009] may serve as a useful test for the various models.

[39] As discussed in section 4 above, there has been debate about the geometry of the subducted Juan de Fuca slab at depth and the nature of possible slab fragmentation in the upper mantle and/or the transition zone [e.g., *Roth et al.*, 2008; *Sigloch et al.*, 2008; *Obrebski et al.*, 2010; *Sigloch*, 2011; *James et al.*, 2011]. The strong, coherent SKS splitting observed beneath the HLP province [*Long et al.*, 2009] and the general pattern of upper mantle seismic anisotropy beneath the PNW [*Fouch and West*, 2008] can be used to make an argument about the likely coherence of the slab in the upper mantle. We have documented an excellent match between the finite strain alignments predicted from a rollback-controlled subduction model with a rigid, coherent slab and the SKS observations beneath eastern Oregon, as discussed in *Druken et al.* [2011] and shown in Figure 5. No alternative explanation for the robust observation of strong, coherent asthenospheric anisotropy with E-W fast directions beneath the HLP has been suggested. We argue, therefore, that the Juan de Fuca slab must act as a coherent body that drives toroidal flow in the upper mantle in order to explain the seismic anisotropy patterns in the PNW. This in turn argues against slab fragmentation, at least in the upper mantle. Given the very convincing tomographic evidence for a fragmented slab in the transition zone and uppermost lower mantle [e.g., *Sigloch*, 2011; *James et al.*, 2011], we envision a scenario in which the Juan de Fuca slab is fragmented at depth but acts as a coherent driver for rollback-controlled flow in the upper mantle.

[40] The experimental work of *Druken et al.* [2011], summarized above, demonstrates that the initiation of slab rollback with upper plate extension (though

modest) is associated with a significant pulse of mantle upwelling that may correspond to the Steens/CRB flood basalts and that continued rollback produces a mantle flow field that is consistent with upper mantle anisotropy [*Long et al.*, 2009] and petrologic constraints [*Till*, 2011] beneath the HLP. These relatively simple laboratory modeling scenarios explain the origin and spatiotemporal evolution of the flood basalts and the HLP well as fundamental consequences of subduction-driven flow patterns. As discussed above and in *James et al.* [2011], additional buoyant mantle upwelling is needed to explain the SRP/Y trend. While we argue that it is not necessary to invoke a classical vertical deep mantle plume (that is, a Rayleigh-Taylor instability originating from a thermal boundary layer at the base of the mantle [e.g., *Morgan*, 1971]) as the source of this upwelling, the difference between the subduction-controlled buoyant mantle upwelling invoked here and the "plume" that is often invoked as the cause of SRP/Y volcanism may be at least partially a matter of semantics. If the definition of "plume" is broad enough to include an upwelling (likely sourced from the uppermost lower mantle, given the evidence for the deflection of the 660 km discontinuity beneath Yellowstone [*Schmandt et al.*, 2012]) whose location and timing is controlled by slab fragmentation, then the SRP/Y volcanic trend may indeed be thought of as plume-related. *Faccenna et al.* [2010] touched on this point when they proposed that the subduction-related mantle upwellings explored in their paper might be considered "a new class of plumes."

[41] To summarize, we have proposed a conceptual model for mantle dynamics beneath the PNW over the past ~20 Ma that is capable of explaining both the first-order observations from the HLP Project and the first-order characteristics of post-20 Ma volcanism, including the Steens/CRB flood basalts and the HLP and SRP/Y volcanic tracks. We have focused on explaining four major observations that have resulted from HLP Project efforts: (1) both geodynamical modeling and seismic anisotropy observations indicate that the present-day mantle flow field beneath the HLP is controlled by slab rollback, (2) tomographic images indicate very low uppermost mantle velocities beneath the SRP and, to a lesser extent, beneath the HLP, with a fragmented Juan de Fuca slab in the transition zone, (3) geodynamical models suggest that the initiation of slab rollback and extension at ~17 Ma was accompanied by a major pulse of mantle upwelling, with ongoing upwelling beneath the HLP associated with rollback-controlled mantle flow, and (4) petrological modeling indicates that HLP basalts are produced by shallow adiabatic decompression melting near the base of the seismically imaged crust. Our model emphasizes the importance of subduction-related processes, including slab fragmentation and rollback, in controlling mantle dynamics and surface tectonomagmatism beneath the PNW over the past 20 Ma. Our analysis does not rule out the presence of a mantle plume beneath the region, but it represents an alternative to the classical mantle plume model that only invokes subduction-related processes as the major drivers for mantle dynamics. Any future models that address the details of upwelling (passive or active) beneath the Pacific Northwest in general and the Snake River Plain/Yellowstone in particular must be consistent with the known plate-driven processes that occur, regardless of the possible presence of a deep mantle plume.

Acknowledgments

[42] This work is part of the High Lava Plains Project, with support provided by the NSF Continental Dynamics program through grants EAR-0507248 (MJF), EAR-0506914 (DEJ and RWC), EAR-0507486 (TLG) and EAR-0506857 (CK). MJF acknowledges additional support from the NSF EarthScope Science program through grant EAR-0548288. LSW's participation was supported through NSF grant EAR-0809192, and MDL acknowledges support from an Alfred P. Sloan Research Fellowship. Seismic data from the USArray Transportable Array network and from the HLP Broadband Seismic Experiment were used in this study, and we thank the vast network of people involved in making these experiments a success. We are particularly grateful to the IRIS PASSCAL and DMC programs for enabling the collection, archiving, and distribution of TA and HLP broadband data, and to Jenda Johnson, Steven Golden, the Eastern Oregon Agricultural Research Center, and the many landowners and field volunteers who made the HLP deployment possible. Finally, we are grateful to Claudio Faccenna, Brandon Schmandt, and an anonymous reviewer for thoughtful and constructive comments that greatly improved the manuscript.

References

Atwater, T. M. (1970), Implications of plate tectonics for the Cenozoic evolution of western North America, *Geol. Soc. Am. Bull.*, *81*, 3513–3536, doi:10.1130/0016-7606(1970)81[3513:IOPTFT]2.0.CO;2.

Atwater, T. M., and J. M. Stock (1998), Pacific-North America plate tectonics of the Neogene southwestern United States: An update, *Int. Geol. Rev.*, *40*, 375–402, doi:10.1080/00206819809465216.

Barnes, C. G. (1992), Petrology of monogenetic volcanoes, Mount Bailey area, Cascade Range, Oregon, *J. Volcanol.*

Geotherm. Res., *52*, 141–156, doi:10.1016/0377-0273(92)90137-3.

Becker, T. W. (2012), On recent seismic tomography for the western United States, *Geochem. Geophys. Geosyst.*, *13*, Q01W10, doi:10.1029/2011GC003977.

Becker, T. W., V. Schulte-Pelkum, D. K. Blackman, J. B. Kellogg, and R. J. O'Connell (2006), Mantle flow under the western United States from shear wave splitting, *Earth Planet. Sci. Lett.*, *247*, 235–251, doi:10.1016/j.epsl.2006.05.010.

Bedle, H., and S. van der Lee (2009), Velocity variations beneath North America, *J. Geophys. Res.*, *114*, B07308, doi:10.1029/2008JB005949.

Bina, C. R., and G. R. Helffrich (1994), Phase transition clapeyron slopes and transition zone seismic discontinuity topography, *J. Geophys. Res.*, *99*, 15,853–15,860, doi:10.1029/94JB00462.

Brueseke, M. E., M. T. Hiezler, W. K. Hart, and S. A. Mertzman (2007), Distribution and chronology of Oregon Plateau (USA) flood basalt volcanism: The Steens Basalt revisited, *J. Volcanol. Geotherm. Res.*, *161*, 187–214, doi:10.1016/j.jvolgeores.2006.12.004.

Burdick, S., C. Li, V. Martynov, T. Cox, J. Eakins, T. Mulder, L. Astiz, F. L. Vernon, G. L. Pavlis, and R. D. van der Hilst (2008), Upper mantle heterogeneity beneath North America from traveltime tomography with global and USArray transportable array data, *Seismol. Res. Lett.*, *79*, 384–392, doi:10.1785/gssrl.79.3.384.

Burdick, S., R. D. van der Hilst, F. L. Vernon, V. Martynov, T. Cox, J. Eakins, G. H. Karasu, J. Tylell, L. Astiz, and G. L. Pavlis (2012), Model update March 2011: Upper mantle heterogeneity beneath North America from traveltime tomography with global and USArray transportable array data, *Seismol. Res. Lett.*, *83*, 23–28, doi:10.1785/gssrl.83.1.23.

Camp, V. E., and B. B. Hanan (2008), A plume-triggered delamination origin for the Columbia River Basalt Group, *Geosphere*, *4*, 480–495, doi:10.1130/GES00175.1.

Camp, V. E., and M. E. Ross (2004), Mantle dynamics and genesis of mafic magmatism in the intermontane Pacific Northwest, *J. Geophys. Res.*, *109*, B08204, doi:10.1029/2003JB002838.

Cao, A., and A. Levander (2010), High-resolution transition zone structures of the Gorda Slab beneath the western United States: Implication for deep water subduction, *J. Geophys. Res.*, *115*, B07301, doi:10.1029/2009JB006876.

Carlson, R. W. (1984), Isotopic constraints on Columbia River flood basalt genesis and the nature of the subcontinental mantle, *Geochim. Cosmochim. Acta*, *48*, 2357–2372, doi:10.1016/0016-7037(84)90231-X.

Carlson, R. W., and W. K. Hart (1987), Crustal genesis on the Oregon Plateau, *J. Geophys. Res.*, *92*, 6191–6206, doi:10.1029/JB092iB07p06191.

Carlson, R. W., D. E. James, M. J. Fouch, T. L. Grove, W. K. Hart, A. L. Grunder, R. A. Duncan, G. R. Keller, S. H. Harder, and C. R. Kincaid (2005), One the cause of voluminous magmatism in the northwestern United States, *Geol. Soc. Am. Abstr. Programs*, *37*, 125.

Christiansen, R. L., and P. W. Lipman (1972), Evolution of the western United States. II: Late Cenozoic, *Philos. Trans. R. Soc. London, Ser. A*, *271*, 249–284, doi:10.1098/rsta.1972.0009.

Christiansen, R. L., G. R. Foulger, and J. R. Evans (2002), Upper-mantle origin of the Yellowstone hotspot, *Geol. Soc. Am. Bull.*, *114*, 1245–1256, doi:10.1130/0016-7606(2002)114<1245:UMOOTY>2.0.CO;2.

Conder, J. A., D. A. Wiens, and J. Morris (2002), On the decompression melting structure at volcanic arcs and back-arc spreading centers, *Geophys. Res. Lett.*, *29*(15), 1727, doi:10.1029/2002GL015390.

Courtier, A. M., et al. (2007), Correlation of seismic and petrologic thermometers suggests deep thermal anomalies beneath hotspots, *Earth Planet. Sci. Lett.*, *264*, 308–316, doi:10.1016/j.epsl.2007.10.003.

Cross, T. A., and R. H. Pilger (1978), Constraints on absolute motion and plate interaction inferred from Cenozoic igneous activity in the western United States, *Am. J. Sci.*, *278*, 865–902, doi:10.2475/ajs.278.7.865.

Currie, C. A., J. F. Cassidy, R. Hyndman, and M. G. Bostock (2004), Shear wave anisotropy beneath the Cascadia subduction zone and western North American craton, *Geophys. J. Int.*, *157*, 341–353, doi:10.1111/j.1365-246X.2004.02175.x.

Deuss, A. (2007), Seismic observations of transition-zone discontinuities beneath hotspot locations, *Spec. Pap. Geol. Soc. Am.*, *430*, 121–136.

Donnelly Nolan, J. M., and T. L. Grove (2009), What is Newberry Volcano?, *Geol. Soc. Am. Abstr. Programs*, *41*, 63.

Druken, K. A., C. Kincaid, and R. W. Griffiths (2009), Laboratory models of three-dimensional mantle flow: Implications on Northwest US volcanism for plume and non-plume sources, *Eos Trans. AGU*, *90*(52), Fall Meet. Suppl., Abstract V53A-05.

Druken, K. A., C. Kincaid, and R. W. Griffiths (2010), Rollback subduction: The great killer of mantle plumes, Abstract U44A-06 presented at 2010 Fall Meeting, AGU, San Francisco, Calif., 13–17 Dec.

Druken, K. A., M. D. Long, and C. Kincaid (2011), Patterns in seismic anisotropy driven by rollback subduction beneath the High Lava Plains, *Geophys. Res. Lett.*, *38*, L13310, doi:10.1029/2011GL047541.

Eagar, K. C., M. J. Fouch, and D. E. James (2010), Receiver function imaging of upper mantle complexity beneath the Pacific Northwest, United States, *Earth Planet. Sci. Lett.*, *297*, 141–153, doi:10.1016/j.epsl.2010.06.015.

Eagar, K. C., M. J. Fouch, D. E. James, and R. W. Carlson (2011), Crustal structure beneath the High Lava Plains of eastern Oregon and surrounding regions from receiver function analysis, *J. Geophys. Res.*, *116*, B02313, doi:10.1029/2010JB007795.

Eakin, C. M., M. Obrebski, R. M. Allen, D. C. Boyarko, M. R. Brudzinski, and R. Porritt (2010), Seismic anisotropy beneath Cascadia and the Mendocino triple junction: Interaction of the subducting slab with mantle flow, *Earth Planet. Sci. Lett.*, *297*, 627–632, doi:10.1016/j.epsl.2010.07.015.

Faccenna, C., T. W. Becker, S. Lallemand, Y. Lagabrielle, F. Funiciello, and C. Piromallo (2010), Subduction-triggered magmatic pulses: A new class of plumes?, *Earth Planet. Sci. Lett.*, *299*, 54–68, doi:10.1016/j.epsl.2010.08.012.

Fouch, M. J. (2012), The Yellowstone hotspot: Plume or not?, *Geology*, *40*, 479–480, doi:10.1130/focus052012.1.

Fouch, M. J., and J. D. West (2008), High resolution imaging of the mantle flow field beneath western North America, *Eos Trans. AGU*, *89*(53), Fall. Meet. Suppl., Abstract U53C-06.

Funiciello, F., M. Moroni, C. Piromallo, C. Faccenna, A. Cenedese, and H. A. Bui (2006), Mapping mantle flow during retreating subduction: Laboratory models analyzed by feature tracking, *J. Geophys. Res.*, *111*, B03402, doi:10.1029/2005JB003792.

Gaetani, G., and T. L. Grove (1998), The influence of water melting on melting of mantle peridotite, *Contrib. Mineral. Petrol.*, *131*, 323–346, doi:10.1007/s004100050396.

Gao, H., E. D. Humphreys, H. Yao, and R. D. van der Hilst (2011), Crust and lithosphere structure of the northwestern US with ambient noise tomography: Terrane accretion and Cascade arc development, *Earth Planet. Sci. Lett.*, *304*, 202–211, doi:10.1016/j.epsl.2011.01.033.

Graham, D. W., M. R. Reid, B. T. Jordan, A. L. Grunder, W. P. Leeman, and J. E. Lupton (2009), Mantle source provinces beneath the northwestern USA delimited by helium isotopes in young basalts, *J. Volcanol. Geotherm. Res.*, *188*, 128–140, doi:10.1016/j.jvolgeores.2008.12.004.

Griffiths, R. W., R. I. Hackney, and R. D. van der Hilst (1995), A laboratory investigation of effects of trench migration on the descent of subducted slabs, *Earth Planet. Sci. Lett.*, *133*, 1–17, doi:10.1016/0012-821X(95)00027-A.

Gripp, A. E., and R. G. Gordon (2002), Young tracks of hotspots and current plate velocities, *Geophys. J. Int.*, *150*, 321–361, doi:10.1046/j.1365-246X.2002.01627.x.

Gromme, C. S., M. E. Beck, R. E. Wells, and D. C. Engebretson (1986), Paleomagnatism of the Tertiary Clarno Formation of central Oregon and its significance for the tectonic history of the Pacific Northwest, *J. Geophys. Res.*, *91*, 14,089–14,103, doi:10.1029/JB091iB14p14089.

Grove, T. L., J. Barr, C. Till, J. D. Donnelly Nolan, and R. W. Carlson (2009), Hot shallow melting in the High Lava Plains, Oregon, *Geol. Soc. Am. Abstr. Programs*, *41*, 571.

Hales, T. C., D. L. Abt, E. D. Humphreys, and J. J. Roering (2005), A lithospheric instability origin for Columbia River flood basalts and Wallowa Mountains uplift in northeast Oregon, *Nature*, *438*, 842–845, doi:10.1038/nature04313.

Hall, P. S., L. B. Cooper, and T. Plank (2012). Thermochemical evolution of the sub-arc mantle due to back-arc spreading, *J. Geophys. Res.*, *117*, B02201, doi:10.1029/2011JB008507.

Hanson-Hedgecock, S., L. S. Wagner, M. J. Fouch, and D. E. James (2012), Constraints on the causes of mid-Miocene volcanism in the Pacific Northwest US from ambient noise tomography, *Geophys. Res. Lett.*, *39*, L05301, doi:10.1029/2012GL051108.

Hart, W. K., J. L. Aronson, and S. A. Mertzman (1984), Areal distribution and age of low-K, high-alumina olivine tholeiite magmatism in the northwestern Great Basin, *Geol. Soc. Am. Bull.*, *95*, 186–195, doi:10.1130/0016-7606(1984)95<186:ADAAOL>2.0.CO;2.

Hebert, L. B., P. Antoshenchkina, P. Asimov, and M. Gurnis (2009), Emergence of a low-viscosity channel in subduction zones through the coupling of mantle flow and thermodynamics, *Earth Planet. Sci. Lett.*, *278*, 243–256, doi:10.1016/j.epsl.2008.12.013.

Herzberg, C., and E. Gazel (2009), Petrological evidence for secular cooling in mantle plumes, *Nature*, *458*, 619–622, doi:10.1038/nature07857.

Hooper, P. R., V. E. Camp, S. P. Reidel, and M. E. Ross (2007), The origin of the Columbia River flood basalt province: Plume versus nonplume models, in *Plates, Plumes, and Planetary Processes*, edited by G. R. Foulger and D. M. Jurdy, *Spec. Pap. Geol. Soc. Am.*, *430*, 635–668.

Humphreys, E. D. (2009), Relation of flat subduction to magmatism and deformation in the western United States, *Mem. Geol. Soc. Am.*, *204*, 85–98.

Humphreys, E. D., and D. D. Coblentz (2007), North American dynamics and western U.S. tectonics, *Rev. Geophys.*, *45*, RG3001, doi:10.1029/2005RG000181.

Humphreys, E. D., K. G. Deuker, D. L. Schutt, and R. B. Smith (2000), Beneath Yellowstone: Evaluating plume and nonplume models using teleseismic images of the upper mantle, *GSA Today*, *10*, 1–7.

James, D. E., M. J. Fouch, R. W. Carlson, and J. B. Roth (2011), Slab fragmentation, edge flow and the origin of the Yellowstone hotspot track, *Earth Planet. Sci. Lett.*, *311*, 124–135, doi:10.1016/j.epsl.2011.09.007.

Jensen, R. A., J. M. Donnelly Nolan, and D. McKay (2009), A field guide to Newberry Volcano, Oregon, in *Volcanoes to Vineyards: Geologic Field Trips Through the Dynamic Landscape of the Pacific Northwest*, edited by J. E. O'Connor et al., *GSA Field Guides*, *15*, 53–79, doi:10.1130/2009.fld015(03).

Jordan, B. T. (2005), Age-progressive volcanism of the Oregon High Lava Plains: Overview and evaluation of tectonic models, *Spec. Pap. Geol. Soc. Am.*, *388*, 503–515.

Jordan, B. T., A. L. Grunder, R. A. Duncan, and A. L. Deino (2004), Geochronology of age-progressive volcanism of the Oregon High Lava Plains: Implications for the plume interpretation of Yellowstone, *J. Geophys. Res.*, *109*, B10202, doi:10.1029/2003JB002776.

Kincaid, C., and R. W. Griffiths (2003), Laboratory models of the thermal evolution of the mantle during rollback subduction, *Nature*, *425*, 58–62, doi:10.1038/nature01923.

Kincaid, C., and R. W. Griffiths (2004), Variability in flow and temperatures within mantle subduction zones, *Geochem. Geophys. Geosyst.*, *5*, Q06002, doi:10.1029/2003GC000666.

Kincaid, C., and P. S. Hall (2003), Role of back arc spreading in circulation and melting at subduction zones, *J. Geophys. Res.*, *108*(B5), 2240, doi:10.1029/2001JB001174.

Kincaid, C., and P. Olson (1987), An experimental study of subduction and slab migration, *J. Geophys. Res.*, *92*, 13,832–13,840, doi:10.1029/JB092iB13p13832.

Kincaid, C., and S. Sacks (1997), Thermal and dynamical evolution of upper mantle in subduction zones, *J. Geophys. Res.*, *102*, 12,295–12,315, doi:10.1029/96JB03553.

Kincaid, C. R., K. A. Druken, R. W. Griffiths, M. D. Long, M. D. Behn, and G. Hirth (2009), Modeling mantle circulation and density distributions in subduction zones: Implications for seismic studies, *Eos Trans. AGU*, *90*(52), Fall Meet. Suppl., Abstract S14A-04.

Leeman, W. P., J. S. Oldow, and W. K. Hart (1992), Lithosphere-scale thrusting in the western U.S. Cordillera as constrained by Sr and Nd isotopic transitions in Neogene volcanic rocks, *Geology*, *20*, 63–66, doi:10.1130/0091-7613(1992)020<0063:LSTITW>2.3.CO;2.

Lin, F.-C., M. H. Ritzwoller, Y. Yang, M. P. Moschetti, and M. J. Fouch (2011), Complex and variable crustal and uppermost mantle seismic anisotropy in the western United States, *Nat. Geosci.*, *4*, 55–61, doi:10.1038/ngeo1036.

Liu, L., and D. R. Stegman (2011), Segmentation of the Farallon slab, *Earth Planet. Sci. Lett.*, *311*, 1–10, doi:10.1016/j.epsl.2011.09.027.

Liu, L., and D. R. Stegman (2012), Columbia River flood basalt formation due to propagating rupture of the Farallon slab, *Nature*, *482*, 386–389, doi:10.1038/nature10749.

Long, M. D., and T. W. Becker (2010), Mantle dynamics and seismic anisotropy, *Earth Planet. Sci. Lett.*, *297*, 341–354, doi:10.1016/j.epsl.2010.06.036.

Long, M. D., H. Gao, A. Klaus, L. S. Wagner, M. J. Fouch, D. E. James, and E. Humphreys (2009), Shear wave splitting and the pattern of mantle flow beneath eastern Oregon, *Earth Planet. Sci. Lett.*, *288*, 359–369, doi:10.1016/j.epsl.2009.09.039.

Long, M. D., M. H. Benoit, M. C. Chapman, and S. D. King (2010), Upper mantle anisotropy and transition zone thickness beneath southeastern North America and implications

for mantle dynamics, *Geochem. Geophys. Geosyst.*, *11*, Q10012, doi:10.1029/2010GC003247.

Magill, J., and A. Cox (1981), Post-Oligocene tectonic rotation of the Oregon Western Cascade Range and the Klamath Mountains, *Geology*, *9*, 127–131, doi:10.1130/0091-7613(1981)9<127:PTROTO>2.0.CO;2.

McCulloch, M. T., and J. A. Gamble (1991), Geochemical and geodynamical constraints on subduction zone magmatism, *Earth Planet. Sci. Lett.*, *102*, 358–374, doi:10.1016/0012-821X(91)90029-H.

Morgan, W. J. (1971), Convection plumes in the lower mantle, *Nature*, *230*, 42–43.

Moschetti, M. P., M. H. Ritzwoller, and N. M. Shapiro (2007), Surface wave tomography of the western United States from ambient seismic noise: Rayleigh wave group velocity maps, *Geochem. Geophys. Geosyst.*, *8*, Q08010, doi:10.1029/2007GC001655.

Müller, R. D., M. Sdrolias, C. Gaina, and W. R. Roest (2008), Age, spreading rates, and spreading asymmetry of the world's ocean crust, *Geochem. Geophys. Geosyst.*, *9*, Q04006, doi:10.1029/2007GC001743.

Niu, F., A. Levander, S. Ham, and M. Obayashi (2005), Mapping the subducting Pacific slab beneath southwest Japan with Hi-net receiver functions, *Earth Planet. Sci. Lett.*, *239*, 9–17, doi:10.1016/j.epsl.2005.08.009.

Norman, M. D., and W. P. Leeman (1990), Open system geochemical evolution of Oligocene subduction-related magmatism, Owyhee Mountains, Idaho, *Chem. Geol.*, *94*, 78–96.

Obrebski, M., R. M. Allen, M. Xue, and S. Hung (2010), Slab-plume interaction beneath the Pacific Northwest, *Geophys. Res. Lett.*, *37*, L14305, doi:10.1029/2010GL043489.

Obrebski, M., R. M. Allen, F. Pollitz, and S.-H. Hung (2011), Lithosphere-asthenosphere interaction beneath the western United States from the joint inversion of body-wave traveltimes and surface-wave phase velocities, *Geophys. J. Int.*, *185*, 1003–1021, doi:10.1111/j.1365-246X.2011.04990.x.

Patro, P. K., and G. D. Egbert (2008), Regional conductivity structure of Cascadia: Preliminary results from 3D inversion of USArray transportable array magnetotelluric data, *Geophys. Res. Lett.*, *35*, L20311, doi:10.1029/2008GL035326.

Pavlis, G. L., K. Sigloch, S. Burdick, M. J. Fouch, and F. Vernon (2012), Unraveling the geometry of the Farallon Plate: Synthesis of three-dimensional imaging results from the USArray, *Tectonophysics*, *532–535*, 82–102, doi:10.1016/j.tecto.2012.02.008.

Pierce, K. L., and L. A. Morgan (1992), The track of the Yellowstone hot spot: Volcanism, faulting and uplift, *Mem. Geol. Soc. Am.*, *179*, 1–53.

Ribe, N. M. (1989), Mantle flow induced by back arc spreading, *Geophys. J. Int.*, *98*, 85–91, doi:10.1111/j.1365-246X.1989.tb05515.x.

Richards, M., R. A. Duncan, and V. E. Courtillot (1989), Flood basalts and hot-spot tracks: Plume heads and tails, *Science*, *246*, 103–107, doi:10.1126/science.246.4926.103.

Robinson, P. T., G. F. Brem, and E. H. McKee (1984), John Day Formation of Oregon: A distal record of early Cascade volcanism, *Geology*, *12*, 229–232, doi:10.1130/0091-7613(1984)12<229:JDFOOA>2.0.CO;2.

Rogers, J. J. W., and J. M. Novitsky-Evans (1977), The Clarno Formation of central Oregon: Volcanism on a thin continental margin, *Earth Planet. Sci. Lett.*, *34*, 56–66, doi:10.1016/0012-821X(77)90105-4.

Roth, J. B., M. J. Fouch, D. E. James, and R. W. Carlson (2008), Three-dimensional seismic velocity structure of the northwestern United States, *Geophys. Res. Lett.*, *35*, L15304, doi:10.1029/2008GL034669.

Rowley, P. D. (1998), Cenozoic transverse zones and igneous belts in the Great Basin, western United States: Their tectonic and economic implications, in *Accommodation Zones and Transfer Zones: The Regional Segmentation of the Basin and Range Province*, edited by J. E. Faults and J. H. Stewart, *Spec. Pap. Geol. Soc. Am.*, *323*, 195–228.

Scarberry, K., A. J. Meigs, and A. L. Grunder (2010), Faulting in a propagating continental rift: Insight from the late Miocene structural development of the Abert Rim fault, southern Oregon, USA, *Tectonophysics*, *488*, 71–86, doi:10.1016/j.tecto.2009.09.025.

Schellart, W. P., D. R. Stegman, and J. Freeman (2008), Global trench migration velocities and slab migration induced upper mantle volume fluxes: Constraints to find an Earth reference frame based on minimizing viscous dissipation, *Earth Sci. Rev.*, *88*, 118–144, doi:10.1016/j.earscirev.2008.01.005.

Schellart, W. P., D. R. Stegman, R. J. Farrington, J. Freeman, and L. Moresi (2010), Cenozoic tectonics of western North America controlled by evolving width of the Farallon slab, *Science*, *329*, 316–319, doi:10.1126/science.1190366.

Schmandt, B., and E. Humphreys (2010), Complex subduction and small-scale convection revealed by body-wave tomography of the western United States upper mantle, *Earth Planet. Sci. Lett.*, *297*, 435–445, doi:10.1016/j.epsl.2010.06.047.

Schmandt, B., K. Dueker, E. Humphreys, and S. Hansen (2012), Hot mantle upwelling across the 660 beneath Yellowstone, *Earth Planet. Sci. Lett.*, *331–332*, 224–236, doi:10.1016/j.epsl.2012.03.025.

Schmerr, N., and C. Thomas (2011), Subducted lithosphere beneath the Kuriles from migration of PP precursors, *Earth Planet. Sci. Lett.*, *311*, 101–111, doi:10.1016/j.epsl.2011.09.002.

Schmidt, M. E., A. L. Grunder, and M. C. Rowe (2008), Segmentation of the Cascade Arc as indicated by Sr and Nd isotopic variation among diverse primitive basalts, *Earth Planet. Sci. Lett.*, *266*, 166–181, doi:10.1016/j.epsl.2007.11.013.

Seedorf, E. (1991), Magmatism, extension and ore deposits of Eocene to Holocene age in the Great Basin–Mutual effects and preliminary proposed genetic relationships, in *Geology and Ore Deposits of the Great Basin*, edited by G. L. Rains and W. H. Wilkinson, pp. 133–178, Geol. Soc. of Nev., Reno.

Severinghaus, J., and T. Atwater (1990), Cenozoic geometry and thermal state of the subducting slabs beneath North America, in *Basin and Range Extensional Tectonics Near the Latitude of Las Vegas, Nevada*, edited by B. P. Wernicke, *Mem. Geol. Soc. Am.*, *176*, 1–22.

Sigloch, K. (2011), Mantle provinces under North America from multi-frequency P wave tomography, *Geochem. Geophys. Geosyst.*, *12*, Q02W08, doi:10.1029/2010GC003421.

Sigloch, K., N. McQuarrie, and G. Nolet (2008), Two-stage subduction history under North America inferred from finite-frequency tomography, *Nat. Geosci.*, *1*, 458–462, doi:10.1038/ngeo231.

Silver, P. G., and W. E. Holt (2002), The mantle flow field beneath western North America, *Science*, *295*, 1054–1057, doi:10.1126/science.1066878.

Smith, R. B., M. Jordan, B. Steinberger, C. M. Puskas, J. Farrell, G. P. Waite, S. Husen, W.-L. Chang, and R. O'Connell (2009), Geodynamics of the Yellowstone hotspot and mantle plume: Seismic and GPS imaging, kinematics, and mantle flow, *J. Volcanol. Geotherm. Res.*, *188*, 26–56, doi:10.1016/j.jvolgeores.2009.08.020.

Smyth, J. R., and S. D. Jacobsen (2006), Nominally anhydrous minerals and Earth's deep water cycle, in *Earth's Deep Water Cycle*, *Geophys. Monogr. Ser.*, vol. 168, edited by S. D. Jacobsen and S. van der Lee, pp. 1–11, AGU, Washington, D. C., doi:10.1029/168GM02.

Spiegelman, M., and D. McKenzie (1987), Models for melt extraction at mid-ocean ridges and island arcs, *Earth Planet. Sci. Lett.*, *83*, 137–152, doi:10.1016/0012-821X(87)90057-4.

Swanson, D. A., T. L. Wright, P. R. Hooper, and R. D. Bentley (1979), Revisions in stratigraphic nomenclature of the Columbia River Basalt Group, *U.S. Geol. Surv. Bull.*, *1457-G*, 1–59.

Takahahshi, E., K. Nakajima, and T. L. Wright (1998), Origin of the Columbia River basalts: Melting model of a heterogeneous plume head, *Earth Planet. Sci. Lett.*, *162*, 63–80, doi:10.1016/S0012-821X(98)00157-5.

Tian, Y., Y. Zhou, K. Sigloch, G. Nolet, and G. Laske (2011), Structure of North American mantle constrained by simultaneous inversion of multiple-frequency SH, SS, and Love waves, *J. Geophys. Res.*, *116*, B02307, doi:10.1029/2010JB007704.

Till, C. B. (2011), Melt generation in the Earth's mantle at convergent plate margins. PhD thesis, 236 pp., Mass. Inst. of Technol., Cambridge.

Till, C. B., T. L. Grove, and M. J. Krawczynski (2012), A melting model for variably depleted and enriched lherzolite in the plagioclase and spinel stability fields, *J. Geophys. Res.*, *117*, B06206, doi:10.1029/2011JB009044.

Tolan, T. L., S. P. Reidel, M. H. Beeson, J. L. Anderson, K. R. Fecht, and D. A. Swanson (1989), Revisions to the estimates of the areal extent and volume of the Columbia River Basalt Group, in *Volcanism and Tectonism in the Columbia River Flood Basalt Province*, edited by S. P. Reidel and P. R. Hooper, *Spec. Pap. Geol. Soc. Am.*, *239*, 1–20.

Trench, D., A. Meigs, and A. Grunder (2012), Termination of northwestern Basin and Range province into a clockwise rotation region of transtension and volcanism, southeast Oregon, *J. Struct. Geol.*, *39*, 52–65, doi:10.1016/j.jsg.2012.03.007.

Wagner, L. S., D. W. Forsyth, M. J. Fouch, and D. E. James (2010), Detailed three-dimensional shear wave velocity structure of the northwestern United States from Rayleigh wave tomography, *Earth Planet. Sci. Lett.*, *299*, 273–284, doi:10.1016/j.epsl.2010.09.005.

Walker, K. T., M. A. H. Hedlin, C. de Groot-Hedlin, J. Vergoz, A. Le Pinchon, and D. P. Drob (2010), Source location of the 19 February 2008 Oregon bolide using seismic networks and infrasound arrays, *J. Geophys. Res.*, *115*, B12329, doi:10.1029/2010JB007863.

Warren, L. M., J. A. Snoke, and D. E. James (2008), S-wave velocity structure beneath the High Lava Plains, Oregon, from Rayleigh-wave dispersion inversion, *Earth Planet. Sci. Lett.*, *274*, 121–131, doi:10.1016/j.epsl.2008.07.014.

Waters, A. C. (1961), Stratigraphy and lithologic variations in the Columbia River Basalt, *Am. J. Sci.*, *259*, 583–611, doi:10.2475/ajs.259.8.583.

Wells, R. E., and P. L. Heller (1988), The relative contribution of accretion, shear, and extension to Cenozoic tectonic rotations in the Pacific Northwest, *Geol. Soc. Am. Bull.*, *100*, 325–338, doi:10.1130/0016-7606(1988)100<0325:TRCOAS>2.3.CO;2.

Wells, R. E., C. S. Weaver, and R. J. Blakely (1998), Fore arc migration in Cascadia and its neotectonic significance, *Geology*, *26*, 759–762, doi:10.1130/0091-7613(1998)026<0759:FAMICA>2.3.CO;2.

Wernicke, B. (1992), Cenozoic extensional tectonics of the U.S. Cordillera, in *The Geology of North America*, vol. G-3, *The Cordilleran Orogen: Conterminous U.S.*, edited by B. C. Burchfiel, P. W. Lipman, and M. L. Zoback, pp. 553–582, Geol. Soc. of Am., Boulder, Colo.

Wernicke, B., G. J. Axen, and J. K. Snow (1988), Basin and Range extensional tectonics at the latitude of Las Vegas, Nevada, *Geol. Soc. Am. Bull.*, *100*, 1738–1757, doi:10.1130/0016-7606(1988)100<1738:BARETA>2.3.CO;2.

West, J. D., M. J. Fouch, J. B. Roth, and L. T. Elkins-Tanton (2009), Vertical mantle flow associated with a lithospheric drip beneath the Great Basin, *Nat. Geosci.*, *2*, 439–444, doi:10.1038/ngeo526.

Wolff, J. A., F. C. Ramos, G. L. Hart, J. D. Patterson, and A. D. Brandon (2008), Columbia River flood basalts from a centralized crustal magmatic system, *Nat. Geosci.*, *1*, 177–180, doi:10.1038/ngeo124.

Xue, M., and R. M. Allen (2010), Mantle structure beneath the western United States and its implications for convection processes, *J. Geophys. Res.*, *115*, B07303, doi:10.1029/2008JB006079.

Yang, Y., and M. H. Ritzwoller (2008), Teleseismic surface wave tomography in the western US using the Transportable Array component of USArray, *Geophys. Res. Lett.*, *35*, L04308, doi:10.1029/2007GL032278.

Yuan, H., and B. Romanowicz (2010), Lithospheric layering in the North American craton, *Nature*, *466*, 1063–1068, doi:10.1038/nature09332.

Zandt, G., and E. Humphreys (2008), Toroidal mantle flow through the western U.S. slab window, *Geology*, *36*, 295–298, doi:10.1130/G24611A.1.